# ANALYSIS OF TRANSIENT OVERVOLTAGE PROTECTION CIRCUITS

FINAL REPORT

DR. RONALD B. STANDLER



U. S. ARMY RESEARCH OFFICE

CONTRACT NUMBER DAAL 03-87-K-0078

THE PENNSYLVANIA STATE UNIVERSITY
ELECTRICAL ENGINEERING DEPARTMENT
COMMUNICATIONS AND SPACE SCIENCES LABORATORY
UNIVERSITY PARK, PA 16802

APPROVED FOR PUBLIC RELEASE;
DISTRIBUTION UNLIMITED.

UNCLASSIFIED
SECURITY CLASSIFICATION OF THIS PAGE

MASTER COPY

FOR REPRODUCTION PURPOSES

# REPORT DOCUMENTATION PAGE

| | |
|---|---|
| 1a. REPORT SECURITY CLASSIFICATION<br>Unclassified | 1b. RESTRICTIVE MARKINGS |
| 2a. SECURITY CLASSIFICATION AUTHORITY | 3. DISTRIBUTION / AVAILABILITY OF REPORT<br>Approved for public release; distribution unlimited. |
| 2b. DECLASSIFICATION / DOWNGRADING SCHEDULE | |
| 4. PERFORMING ORGANIZATION REPORT NUMBER(S) | 5. MONITORING ORGANIZATION REPORT NUMBER(S)<br>ARO 24970.6-EL |
| 6a. NAME OF PERFORMING ORGANIZATION<br>The Pennsylvania State University<br>6b. OFFICE SYMBOL (If applicable) | 7a. NAME OF MONITORING ORGANIZATION<br>U. S. Army Research Office |
| 6c. ADDRESS (City, State, and ZIP Code)<br>Electrical Engineering Department<br>Communications & Space Sciences Laboratory<br>University Park, PA 16802 | 7b. ADDRESS (City, State, and ZIP Code)<br>P. O. Box 12211<br>Research Triangle Park, NC 27709-2211 |
| 8a. NAME OF FUNDING / SPONSORING ORGANIZATION<br>U. S. Army Research Office<br>8b. OFFICE SYMBOL (If applicable) | 9. PROCUREMENT INSTRUMENT IDENTIFICATION NUMBER<br>DAAL 03-87-K-0078 |
| 8c. ADDRESS (City, State, and ZIP Code)<br>P. O. Box 12211<br>Research Triangle Park, NC 27709-2211 | 10. SOURCE OF FUNDING NUMBERS<br>PROGRAM ELEMENT NO. / PROJECT NO. / TASK NO. / WORK UNIT ACCESSION NO. |

11. TITLE (Include Security Classification)
Analysis of Transient Overvoltage Protection Circuits

12. PERSONAL AUTHOR(S)
Dr. Ronald B. Standler

| 13a. TYPE OF REPORT | 13b. TIME COVERED | 14. DATE OF REPORT (Year, Month, Day) | 15. PAGE COUNT |
|---|---|---|---|
| Final | FROM Aug 87 TO Jun 90 | June 1990 | -- |

16. SUPPLEMENTARY NOTATION
The view, opinions and/or findings contained in this report are those of the author(s) and should not be construed as an official Department of the Army position, policy, or decision, unless so designated by other documentation.

| 17. COSATI CODES | | |
|---|---|---|
| FIELD | GROUP | SUB-GROUP |
| | | |
| | | |

18. SUBJECT TERMS (Continue on reverse if necessary and identify by block number)
Electromagnetic pulse
Terminal Protection Devices

19. ABSTRACT (Continue on reverse if necessary and identify by block number)

This report reviews the work performed during a research contract to study terminal protection devices (TPDs) for protecting electronic systems from damage by transient overvoltages. Analytical mathematical relations are given for standard surge test waveforms and the output of commercial surge generators are compared with these equations.

Low-pass filters for use on the ac supply mains are evaluated as TPDs.

A TPD for a system with a wide signal bandwidth (dc to 200 MHz) is discussed. Computation of energy in a surge from measurements of voltage alone across an unknown load is shown to be invalid. Nonlinear series devices are considered briefly.

| | |
|---|---|
| 20. DISTRIBUTION / AVAILABILITY OF ABSTRACT<br>☒ UNCLASSIFIED/UNLIMITED ☐ SAME AS RPT. ☐ DTIC USERS | 21. ABSTRACT SECURITY CLASSIFICATION<br>Unclassified |
| 22a. NAME OF RESPONSIBLE INDIVIDUAL | 22b. TELEPHONE (Include Area Code) / 22c. OFFICE SYMBOL |

DD FORM 1473, 84 MAR

83 APR edition may be used until exhausted.
All other editions are obsolete.

SECURITY CLASSIFICATION OF THIS PAGE
UNCLASSIFIED

## INTRODUCTION

This project was a three-year effort to examine several fundamental issues in protecting electronic circuits from damage by transient overvoltages caused by lighting and detonation of nuclear weapons (EMP). The work in the proposal was divided into three areas: (1) numerical analysis of nonlinear equations that describe fundamental protection circuits, (2) investigation of reflection, transmission, and absorption of energy by transient protection circuits, and (3) investigation of nonlinear series elements for overvoltage protection circuits.

This research project was funded one year at a time with money from the U.S. Army Harry Diamond Laboratories. It was necessary to shift the goals and topics of this research project each year in order to match the sponsor's program.

### first year (Aug 1987--Aug 1988)

The principal topic during the first year of this project was a review of ways to make spark gaps conduct in subnanosecond times. This effort was completed in March 1988 and described in an Army report[1].

Traditional surge (overvoltage) waveforms are defined with just three points: two points on the leading edge of the wave and one point on the tail. Such a crude definition is inadequate for mathematical analysis of surge protection circuits. Therefore, it was necessary to find mathematical representations for the standard surge waveforms that were consistent with the traditional specifications. The results of this research effort was published as a short paper in the IEEE Transactions on Electromagnetic Compatibility and is reprinted in this report. Most of the unipolar

[1]R. B. Standler, "Technology of Fast Spark Gaps," U.S. Army Harry Diamond Laboratories Contractor Report HDL-CR-89-078, 44 pp., Sep 1989.

waveforms could be described as double exponentials, however the 8/20 μs current waveshape can not be described as a sum of two exponential functions. During this work it was discovered that the 100 kHz Ring Wave specified in ANSI C62.41-1980 can not be satisfied with a simple damped cosine waveform. The paper gives a more complicated relation that is continuous everywhere, as well as an "almost satisfactory" damped cosine relation.

The remainder of the first year of this project was devoted to (1) a comparison of different commercially-available laboratory surge generators and (2) a proposal to define surge waveforms with equations, rather than with just three points. The results of this work were presented at the Eighth International Zürich Symposium on Electromagnetic Compatibility, and are reprinted in this report. As a result of this research work, the principal investigator was appointed Chairman of the Task Force that wrote the specification and tolerances for the standard surge test waveforms in ANSI C62.41-199X.

Evaluation of commercially-available surge generators for the 100 kHz Ring Wave showed that three different models of generators did not produce the same waveform. Thus there was a correspondence between (1) a specification that could not be translated into a simple electrical circuit and (2) a lack of reproducibility of laboratory waveforms among different equipment vendors. In other words, the neglect of theoretical considerations (mathematical simplicity) caused a practical problem. Such situations are all too common in engineering. The principal investigator has corrected this situation by inserting the simple damped cosine as the nominal 100 kHz Ring Wave specification into the revision of ANSI C62.41. To prevent making existing generators unacceptable, the principal investigator specified tolerances that would include the waveform from the old specification as well as the new, damped cosine. The principal investigator's proposals have been accepted by the IEEE Power Engineering Society Working Group 3.6.4 that is revising ANSI C62.41. This revision of should be completed and approved in 1990 or 1991.

Use of equations to specify nominal surge waveforms for surge testing

is not only more precise than the traditional three-point specification, but the use of equations with specific numerical values for time constants makes it much easier to design laboratory surge generators, as well as making it possible to do computer-aided design of overvoltage protection circuits.

This work was also noteworthy in that numerical algorithms were developed for objective evaluation of surge waveshapes. As noted in Appendix 2 of the Zürich paper, these algorithms could increase the resolution of the data from the digital oscilloscopes.

Another task completed during the first year of this project was the development of a module that contained both overvoltage protection and a low-pass filter for protection of equipment on the ac supply mains. The results of this work were reported at the IEEE Industry Applications Society Industrial and Commercial Power Conference in 1988. A copy of the conference paper is included in this report. Noteworthy topics in this work are the (1) synergistic actions of voltage clamping and filtering to attenuate disturbances on the mains and (2) the design of a filter that does not form a resonant circuit with realistic load impedances. This paper is one a very few treatments in the archival literature of the role of low-pass filters in overvoltage protection.

second year (Aug 1988--Aug 1989)

Development of circuit models for TPD_components (metal oxide varistors, spark gaps, and avalanche diodes for transient suppression) and their incorporation in the SPICE circuit simulation program was *scheduled* to be the principal effort during the second year of this project. Harry Diamond Laboratory staff insisted on the use of SPICE because they had already sponsored the development of SPICE code and they preferred to add to existing tools, rather than reinvent them. The disadvantage of adding code to SPICE is that the SPICE code is very large: current versions of SPICE require overlays in order to run on an IBM PC desktop computer, even with the maximum 640 kB of memory. Many people have participated in the development of the source code over the last twenty years and the present SPICE program is very sophisticated. Therefore, adding to the SPICE program

is not a minor undertaking. However, in the second year of this project the level of funding was cut to half of the amount in the contract with the Army Research Office due to government-wide budget cuts, which annihilated our circuit analysis work with SPICE.

The principal task during the second year of this project was the development of a novel circuit that met the following criteria:

1. signal bandwidth from dc to at least 100 MHz,
2. impedance matched to a 50 Ω transmission line,
3. survive an 8/20 μs waveshape with a peak current of 3 kA, and
4. have a clamping voltage of less than 20 V across the protected port.

Such a circuit would be useful to protect radio receivers and computer local-area networks from damage by transient overvoltages. This effort was successful. Details are given in a paper that was submitted in Sep 1989 to IEEE Trans. on Electromagnetic Compatibility for review and publication. A draft copy of this paper is included in this report.

Several engineers have calculated the "energy in a surge" from measurements of the voltage, V, and the relationship

$$\int V^2 \, dt$$

The principal investigator analyzed this technique and concluded that it was flawed for a number of different reasons. The analysis was presented at the IEEE National Symposium on Electromagnetic Compatibility in March 1989. A copy of the conference paper from the printed record is included in this report. This work is noteworthy in that SPICE was used to compute current and voltage in a network that was excited by standard surge waveforms.

## nonlinear series devices

Conventional surge protection components are normally nonconducting, but during an overstress they have a resistance of the order of 1 Ω or less. Such devices are placed in shunt with the equipment to be protected. Any solid state device that can tolerate kiloampere surge currents must have a large cross-sectional area, which makes the parasitic capacitance large. This large capacitance makes these devices inappropriate for applications where signal bandwidths of more than 100 kHz are required. Moreover, the

magnetic field from the large surge current can induce destructive voltages in neighboring conducting loops. This insidious side effect of the surge current has been discussed in detail[2]

A nonlinear series device would be a useful addition to the overvoltage protection armamentarium. Such a device would be normally conducting (i.e., resistance less than 10 Ω). During an overstress, the device would have a large resistance (e.g., more than 1 kΩ). Such a series device would limit surge currents to shunt protective devices downstream. In particular, avalanche diodes with a small junction area could be fabricated at the input/output terminals inside an integrated circuit as the final overvoltage protection device.

Nonlinear series devices may also be useful in designing protective circuits against long-duration overstresses, which have durations of at least a few milliseconds. Such overvoltages are commonly produced by switching power-factor correction capacitors on electric power distribution systems or by continuing current in cloud-to-ground lighting flashes that strike overhead power lines. They may also be generated by magneto-hydrodynamic electromagnetic pulses from nuclear weapons. Conventional, economical shunt protective devices can not absorb all of the energy in a long-duration overstress without damage or degradation.

Several different polymer positive temperature coefficient (PTC) resistors were exposed to large surge currents (e.g., 500 A to 3 kA peak, 8/20 μs waveshape) in the principal investigator's laboratory during the second year of this project. All of the samples exploded. Examination of the failed component showed evidence of an arc channel between the sharp ends of the cylindrical electrodes. An invention disclosure was prepared that suggested a modified design by (1) bending the electrodes so that the sharp ends were no longer in a region of intense electric field and (2) placing a ceramic plate between the electrodes to force the current in the

[2]R.B. Standler, Protection of Electronic Circuits from Overvoltages, New York: Wiley-Interscience, pp. 127-128, 209-213.

conductive polymer to have a longer path, which might help avoid an arc channel. The invention disclosure is currently (Nov 1989) being evaluated by the manufacturer of the polymer PTC devices, Raychem Corporation.

A preliminary effort was made to evaluate the use of depletion-mode power MOSFETs as series elements in surge protection circuits. The parasitic diode between the drain and source terminals prevented this device from being useful in simple protection circuits.

third year of project

The principal investigator will move to the University of Kentucky in July 1990 and the third year of this contract will be performed at that institution. At the present time (Nov 1989), severe budget cuts have removed all Harry Diamond Laboratory money that was to be allocated to this project. If funding is restored, work will continue on developing models of overvoltage protection circuits in SPICE and will begin on experimental evaluations of propagation of surges on transmission lines.

In 1987-1988 the principal investigator wrote FORTRAN programs to take the equations for standard surge test waveforms and produce a piecewise linear representation for current (or voltage) that was suitable for inclusion in a SPICE circuit file. This was not a simple task, since there were conflicting requirements:

1. small number of points in the piecewise linear representation,
2. small relative error (< 0.5%) in linear approximation, and
3. small relative error (< 20%) in slope of linear approximation.

The considerable amount of work in the development of these piecewise linear representations was rendered obsolete by a new feature in version 4.0 of PSPICE, which was released in July 1989. In that version of SPICE one can use the .FUNC command and either the E or G model to place analytical expressions in voltage or current sources.

# Equations for Some Transient Overvoltage Test Waveforms

Ronald B. Standler

Reprinted from
IEEE TRANSACTIONS ON ELECTROMAGNETIC COMPATIBILITY
Vol. 30, No. 1, February 1988

# Short Papers

## Equations for Some Transient Overvoltage Test Waveforms

RONALD B. STANDLER, SENIOR MEMBER, IEEE

*Abstract*—**Simple equations are provided that satisfy the definitions of five of the most common transient overvoltage test waveforms: the ringwave specified in ANSI C62.41-1980, the fast transient specified in IEC 801, the 8/20 μs, 1.2/50 μs, and the 10/1000 μs waveforms. These equations are useful for performing computer simulations of the response of electronic circuits to transient overvoltages.**

*Key Words*—**Overvoltage transients, test waveforms.**

*Index Code*—**A99e.**

### I. Introduction

Transient overvoltages, which, for example, may be caused by lightning or switching reactive loads, are a common cause of damage or upset (temporary malfunction) of electronic circuits and systems. It is important to assess the vulnerability of electronic systems to damage and upset by transient overvoltages, as well as to test the adequacy of protective circuits. To this end, standard publications describe several test waveforms that are representative of transient overvoltages [1]-[3]. It was originally envisioned that these standard test waveforms would be used during experiments in a laboratory. More recently, engineers (including the author) have also performed computer simulations of the response of circuits to transient overvoltages.

The standard documents define test waveforms in terms of front time, time to fall to half the peak value, amplitude, and, when appropriate, oscillation frequency. No mathematical relations are given in these standard documents. Equations would be convenient for engineers who wish to perform computer simulations of transient protection circuits. Further, having the time constants (rather than front time and time to half-value) makes it easier to design *RLC* pulse-forming networks (PFN's) for use in laboratory pulse generators.

### II. 100-kHz Ring Waveform

A simple mathematical expression for the 0.5-μs-100-kHz ring wave that is specified in [2] is $V(t)$, as given by (1):

$$V(t) = AV_p\{1 - \exp(-t/\tau_1)\} \exp(-t/\tau_2) \cos(\omega t) \quad (1)$$

where $\tau_1 = 0.5334\ \mu s$, $\tau_2 = 9.788\ \mu s$, $\omega = 2\pi \cdot 10^5\ s^{-1}$, $A = 1.590$, $t$ is the time, and $V_p$ is the maximum or peak value of $V(t)$.

The definition of the ring wave in [2] states that the amplitude decays to 60 percent between adjacent positive and negative peaks. These peaks occur 5 μs apart, except that the first positive and first negative peaks occur about 3.9 μs apart (owing to the rise-time term). The decay of the ring wave in (1) is given by the $\exp(-t/\tau_2)$ term, where the value of $\tau_2$ is determined by

$$\exp(-5\ \mu s/\tau_2) = 0.6.$$

In the representation given by (1), the decay of amplitude between the first positive and first negative peak does not satisfy the definition in [2]. The first negative peak has an amplitude that is 96.7 percent of $V_p$; however, the relative amplitudes of all other peaks are correct. To satisfy the definition with (1) requires that the time constant $\tau_2$ change value between the first and second half-cycles of the waveform. This is not only unphysical, but the methods that I have tried spoiled the ratio of amplitudes of the first negative peak and the second positive peak.

An accurate representation of the ring wave that is defined in [2] can be achieved by using (2):

$$y(t) = A\{1 - \exp(-t/\tau_1)\} \exp(-t/\tau_2) \cos(\omega t)$$

$$V(t) = \begin{cases} BV_p y(1 + \eta y), & 0 \le t \le 2.5\ \mu s \\ BV_p y, & 2.5\ \mu s \le t \end{cases} \quad (2)$$

where $\tau_1 = 0.4791\ \mu s$, $\tau_2 = 9.788\ \mu s$, $\omega = 2\pi \cdot 10^5\ s^{-1}$, $A = 1.590$, $B = 0.6205$, and $\eta = 0.523$. Notice that the value of $\tau_1$ has changed from that given above with (1). While this equation is defined in a piecewise fashion, both $V(t)$ and its derivative are continuous for $t > 0$. The effect of this procedure is to make the first positive peak greater than it was in (1), so that the amplitudes of all of the peaks are correct. A plot of (2) is shown in Fig. 1.

### III. 8/20 μs Waveform

A simple mathematical expression for the 8/20 μs current waveform that is specified in [1]-[3] is $I(t)$, as given by (3):

$$I(t) = AI_p t^k \exp(-t/\tau) \quad (3)$$

where $A = 0.01405\ (\mu s)^{-k}$, $k = 2.93$, $\tau = 3.977\ \mu s$, $t$ is the time in microseconds, and $I_p$ is the peak value of the current. Unfortunately, this expression cannot be integrated analytically to obtain the charge transferred. A good approximation, which can be integrated analytically, results when the constants have the following values: $k = 3.0$, $\tau = 3.911\ \mu s$, and $A = 0.01243\ (\mu s)^{-3}$. A plot of (3) with $k = 3.0$ is shown in Fig. 2.

The $t^3$ approximation gives a front time that is 0.3 percent too large, and a time to half-value that is 0.3 percent too small. However, this small error is outweighed by having an equation for current that can be integrated analytically. The standards [1], [3] specify a tolerance of ±10 percent for both the 8-μs front time and the 20-μs time to half-value, so the 0.3-percent error in using the $t^3$ approximation is well within acceptable limits.

It should be noted that the 8-μs "virtual duration of wavefront" is clearly defined in [1] and [3]. If the initial part of the waveform were a linear function of time (it is not), then the virtual duration of the wavefront would be the time between the initial zero and the peak, or crest, of the waveform.

### IV. 1.2/50 μs Waveform

The 1.2/50 μs voltage waveform that is specified in [1]-[3] is $V(t)$, as given by (4):

$$V(t) = AV_p\{1 - \exp(-t/\tau_1)\} \exp(-t/\tau_2) \quad (4)$$

where $\tau_1 = 0.4074\ \mu s$, $\tau_2 = 68.22\ \mu s$, $A = 1.037$, $t$ is the time, and $V_p$ is the peak value of $V(t)$. The standards [1], [3] specify that a tolerance of ±30 percent applies to the 1.2-μs front time and a

Manuscript received January 15, 1987; revised October 10, 1987.

The author is with the Department of Electrical Engineering, Pennsylvania State University, University Park, PA 16802. Tel. (814) 863-1470.

IEEE Log Number 8718467.

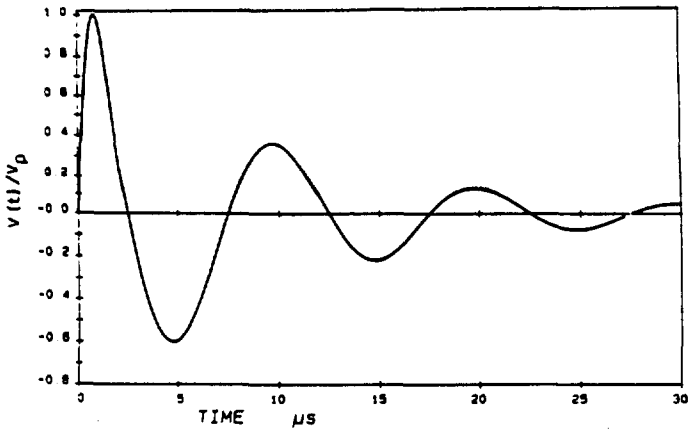


Fig. 1. 0.5-μs–100-kHz ring wave.

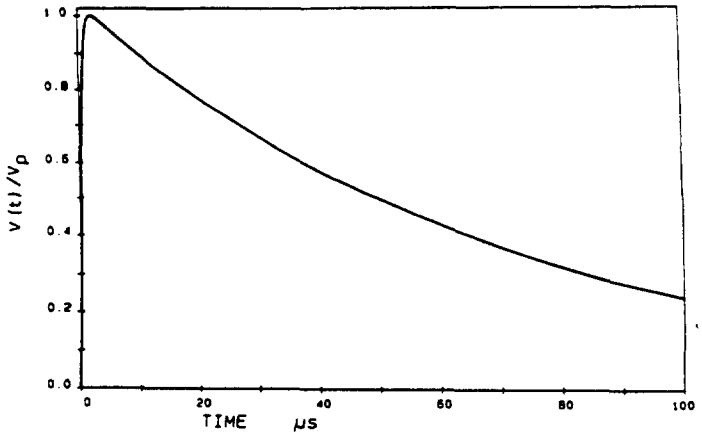


Fig. 3. 1.2/50 μs.

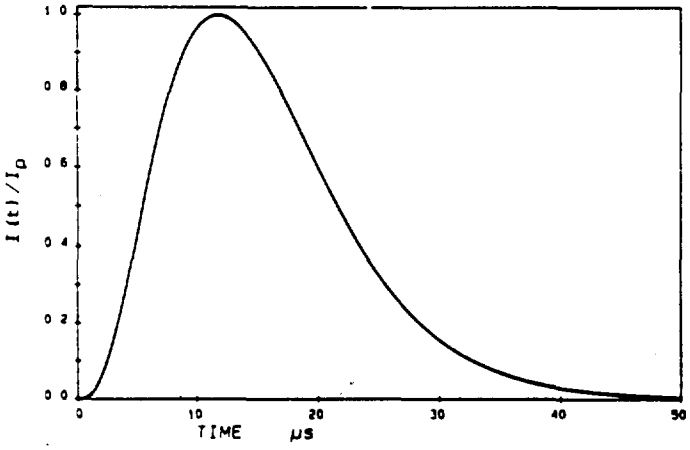


Fig. 2. 8/20 μs.

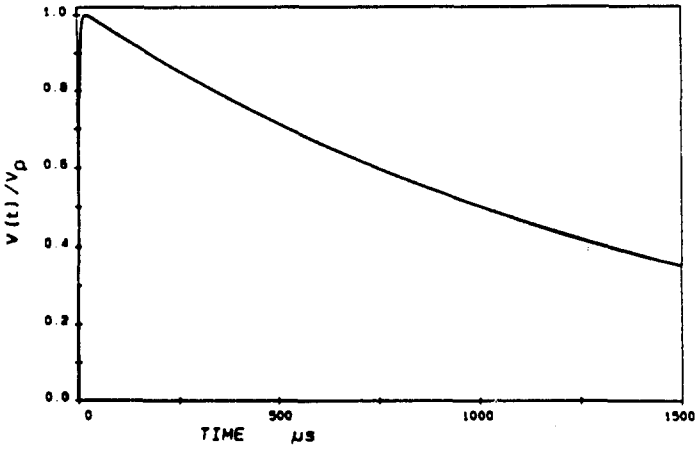


Fig. 4. 10/1000 μs.

tolerance of ±20 percent applies to the 50-μs time to half-value. A plot of (4), with the parameters for a 1.2/50 μs waveform, is shown in Fig. 3.

## V. 10/1000 μs Waveform

The 10/1000 μs waveform represents transient overvoltages that appear on telephone lines during thunderstorms [4], [5]. While it is obvious from the designation "10/1000 μs" that the "front time" has a duration of 10 μs, it is not clear how this word is properly defined for this waveform. Three different definitions have been used. Bodle and Gresh [4] appear to have used the word "front time" to indicate the time between the initial zero and the peak value. As a second definition, Bennison *et al.* [5] used the standard definition of "rise time" in electronic engineering, the time interval between the 10- and 90-percent points of the waveform. The third definition, which is present Bell Communications practice [6], is to use 1.25 times the interval between the 10- and 90-percent points on the leading edge of the waveform as the 10-μs front time. This last definition is the same as that used for the 8/20 μs waveform [1], [3] and is consistent with common high-voltage laboratory practice. A simple expression for this voltage waveform, with the third definition of front time, is $V(t)$, as given by (5):

$$V(t) = A V_p \{1 - \exp(-t/\tau_1)\} \exp(-t/\tau_2) \qquad (5)$$

where $\tau_1 = 3.827$ μs, $\tau_2 = 1404$ μs, $A = 1.019$, $t$ is the time, and $V_p$ is the peak value of $V(t)$. A plot of (5), with these parameters for a 10/1000 μs waveform, is shown in Fig. 4.

The 10/1000 μs waveform may also be represented by the piecewise continuous expression that is given in (6):

$$V(t) = \begin{cases} (V_p/10\ \mu s)t, & \text{for } 0 \leqq t \leqq 10\ \mu s \\ V_p \exp(-(t-10\ \mu s)/1428\ \mu s), & \text{for } t > 10\ \mu s. \end{cases} \qquad (6)$$

While the piecewise representation is advocated in [4], it has the disadvantage of having a discontinuity in the derivative at $t = 10$ μs, while the double exponential model has continuous derivatives of all orders. For this reason, I favor the use of (5) instead of (6).

## VI. IEC EFT 5/50 ns Waveform

Recently, the IEC has defined an "electrical fast transient" (EFT) test waveform that has a 5/50 ns shape [7]. A simple mathematical expression for this waveform is $V(t)$, as given by (7):

$$V(t) = A V_p \{1 - \exp(-t/\tau_1)\} \exp(-t/\tau_2) \qquad (7)$$

where $\tau_1 = 3.5$ ns, $\tau_2 = 55.6$ ns, $A = 1.270$, $t$ is the time, and $V_p$ is the peak value of $V(t)$. The standard specifies tolerances of ±30 percent for both the 5-ns rise time and 50-ns duration. A plot of (7), with the parameters for the EFT, is shown in Fig. 5.

## VII. Conclusion

A plot of three overvoltage test waveforms is shown in Fig. 6. The EFT waveform is not shown in Fig. 6 because, on this scale, it would be a vertical line at $t = 0$. The 8/20 μs waveform is also not shown in Fig. 6 because it is a current waveform, not a voltage waveform. As shown by Figs. 4 and 6, the 10/1000 μs waveform provides a relatively long duration unipolar stress. The 1.2/50 μs waveform and the 8/20 μs current waveform are shorter duration unipolar stresses.

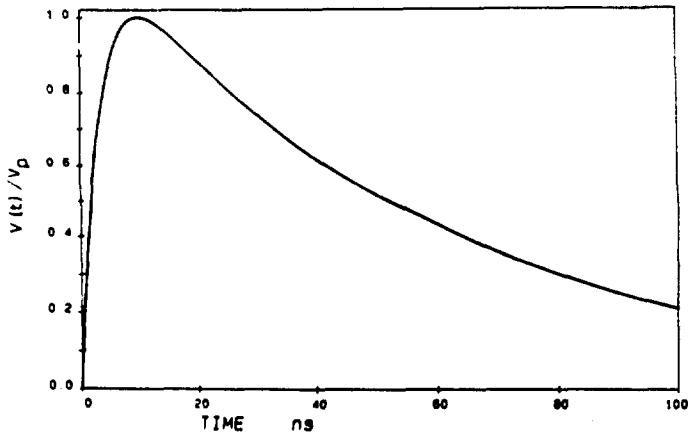


Fig. 5. IEC 801 EFT.

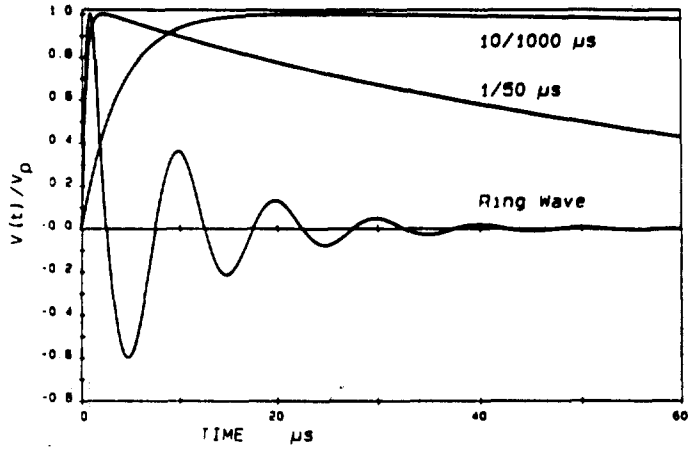


Fig. 6. Various overvoltage test waveforms.

The 0.5-μs-100-kHz ring wave is the only oscillatory waveform in the collection of test waveforms reported in this paper.

A test waveform in the laboratory, of course, will not exactly match the waveform given by these equations due to loading by the device under test. The tolerances of components in PFN's and the parasitic inductances and capacitances in components in both the PFN and test fixture may cause additional discrepancy. Several of the standards, as noted above, specify tolerances between ±10 and ±30 percent for the front time and time to half-value. The output of a surge generator of unipolar waves is unacceptable only if its rise time or time to half-value fails to meet the criteria specified in the appropriate standard.

There does not appear to be a simple mathematical definition for the ringwave that agrees with the definition in ANSI Standard C62.41-1980. This document is now being revised, and I hope to modify the definition slightly.

## Acknowledgment

The author thanks P. Richman and F. Martzloff for their suggestions.

## References

[1] *IEEE Standard Techniques for High-Voltage Testing*, ANSI Standard 4-1978.

[2] *IEEE Guide for Surge Voltages in Low-Voltage AC Power Circuits*, ANSI Standard C62.41-1980 (formerly IEEE Standard 587).

[3] *IEEE Standard for Surge Arresters for AC Power Circuits*, ANSI Standard C62.1-1984 (formerly IEEE Standard 28-1974).

[4] D. W. Bodle and P. A. Gresh, "Lightning surges in paired telephone cable facilities," *Bell System Tech. J.*, vol. 40, pp. 547-576, Mar. 1961.

[5] E. Bennison, A. J. Ghazi, and P. Ferland, "Lightning surges in open wire, coaxial, and paired cables," *IEEE Trans. Commun.*, vol. COM-21, pp. 1136-1143, Oct. 1973.

[6] "Lightning and 60 Hz disturbances at the Bell Operating Company "network interface," Bell Commun. Res., Morristown, NJ, Rep. TR-EOP-000 001, June 1984.

[7] "Electromagnetic compatibility for industrial-process measurement and control equipment—Part 4: Electrical fast transient/burst requirements," Int. Electrotech. Commission, Geneva, Switzerland, Rep. 801-4, 1987.

# STANDARD WAVEFORMS FOR SURGE TESTING:

# EXPERIMENTAL EVALUATION AND PROPOSED NEW CRITERIA FOR TOLERANCES

Ronald B. Standler

The Pennsylvania State University

University Park, PA U.S.A.

An experimental evaluation was conducted to compare waveforms from high-voltage surge generators to the waveform specifications. Generators from three major manufacturers were evaluated for (1) the combination 1.2/50 μs voltage and 8/20 μs current waveform and (2) the 100 kHz ring wave specified in ANSI C62.41-1980. Changes in the waveform when the surge generator was connected to metal-oxide varistors or a 0.1 μF capacitor were also described. Finally, proposals are made for more complete specifications for the 1.2/50 and 8/20 μs waveforms.

## Introduction

Transient overvoltages, which, for example, may be caused by lightning or switching reactive loads, are a common cause of damage or upset (temporary malfunction) of electronic circuits and systems. It is important to assess the vulnerability of electronic systems to damage and upset by transient overvoltages, as well as to test the adequacy of protective circuits. Standard publications specify the traditional 1.2/50 μs voltage impulse and the 8/20 μs current waveform in references [1,2] and the newer 100 kHz ring waveform in [3] as representative of surges on ac supply mains. Standard waveforms are defined only for an ideal load: either an open-circuit for voltage waveforms or a short-circuit for current waveforms. The behavior of the surge waveforms under other types of loads, e.g., varistors or capacitors, is unspecified.

Part I of this paper reports how well several commercially available surge generators meet the specifications for the 1.2/50 and 8/20 μs and 100 kHz ring waveforms. Part II of this paper examines the effects of three different loads on the voltage and current waveforms. Part III of this paper suggests more comprehensive specifications for adequate surge testing waveforms.

The specifications for the 1.2/50 μs and 8/20 μs waveforms contain tolerances for the front time, duration, and peak value that define these waveforms. Part I of this paper is useful as a routine review of the performance of the 1.2/50 μs and 8/20 μs waveform generators. There are no specified tolerances for the parameters of the 100 kHz ring waveform. F.D. Martzloff, the Chairman of the Working Group that is presently revising ANSI C62.41-1980 [3], has proposed adding tolerances to the 100 kHz ring wave in the revised version. Part I of this paper is useful to assist in setting tolerances on the 100 kHz ring wave: It is important that tolerances in future versions of standards not make existing ring wave surge generators unacceptable. If we could avoid making a model of a commercial 100 kHz ring wave generator unacceptable by specifying tolerances of, for example, ±20% instead of ±10%, then it would be desirable to accept the slightly broader tolerance in the revised version of ANSI C62.41.

## Present Specifications for Waveforms

The unipolar waveforms considered in this paper are specified by giving the front time, duration, and peak value. Fig. 1 shows a typical unipolar *current* waveform and three points, $t_1$, $t_2$, and $t_3$ that occur at the 10% and 90% points on the leading edge and the 50% point on the tail. The virtual origin, $t_0$, is the time that a straight line through the 10% and 90% points on the leading edge of the surge reaches zero current. The front time, $t_f$, and duration, $t_d$, are defined by

$$t_f = 1.25\ (t_2 - t_1) \quad (1)$$

$$t_d = t_3 - t_0 \quad (2)$$

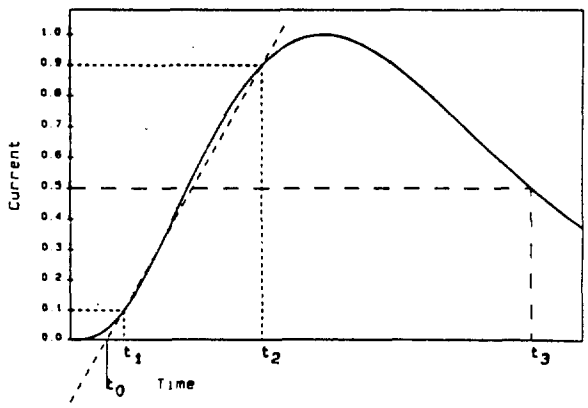


Fig. 1 Pictorial definition of points on a unipolar waveform that are used to define the front time and duration.

For a unipolar *voltage* waveform, the same procedure is used except that the value of $t_1$ is determined at the 30% point on the leading edge and the front time is determined by

$$t_f = 1.67\ (t_2 - t_1) \qquad (3)$$

The historical reasons for these specifications are given in [4].

The specifications for the 8/20 μs current waveform call for tolerances of ± 10% on the 8 μs front time, 20 μs duration, and peak value. The specifications for the 1.2/50 μs wave call for a front time of 1.2 μs ± 30%, a duration of 50 μs ± 20%. The peak voltage is to be specified within ± 3%.

The 100 kHz ring wave is specified by a 0.5 μs rise time of the leading edge, and a 10 μs period for the oscillation. The rate of decay of the oscillation is specified by stating that the ratio of amplitude is 60% for adjacent peaks of opposite polarity. The rise time has the usual definition in electrical engineering, the time difference between the 90% and 10% points on the leading edge of the waveform. There is no factor of 1.25 or 1.67 in the definition of rise time, which distinguishes "rise time" from "front time". There are no tolerances in the specification for this ring wave.

## PART I: Experimental Results

Several commercially available surge generators were obtained and the output voltage and current were measured with digital oscilloscopes for each of the following waveforms. Generators A, B, C provided the combination 1.2/50 μs voltage wave and 8/20 μs current waveform. Generator D provided the 8/20 μs current waveform. Generators P, Q, R provided the 100 kHz ring waveform. Most of these surge generators were loaned by their manufacturers (Haefely, KeyTek, Velonex) on the condition that the performance of specific models of generators not be identified. All seven generators are presently being manufactured, none are obsolete.

Fig. 2 shows the connection of the surge generator, the load, and the measuring instruments. A pair of digital oscilloscopes were used to measure the voltages and currents. Details of the instrumentation are given in Appendix I.

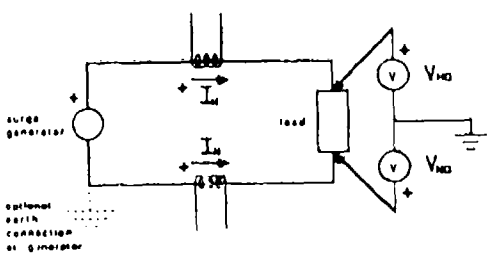


Fig. 2 Schematic diagram of apparatus.

Generators B, Q, and R were used with the back filter supplied by the manufacturer. For short-circuit testing of generators B and R, the mains were disconnected. For other loading of generators B and R, the mains were connected and the surges were applied when the instantaneous value of the mains voltage was zero. For all measurements with generator Q the three conductors (hot, neutral, and earth) were connected together on the mains side of the back filter to simulate the small impedance of the mains. The other surge generators were designed to give the proper waveform without a back filter, and were tested without a back filter. These different test situations were required by the design of the surge generators and the specific cables that were supplied by the manufacturer.

Specifications for overvoltage test waveforms are given for idealized loads: voltage waveforms are specified for an open-circuit load, current waveforms are specified for a short-circuit load. Therefore, only open-circuit and short-circuit loads were used for this part of the experiment.

Because the voltage across the energy storage capacitor inside the surge generator may be proportional to the rms mains voltage, a ferroresonant line conditioner was used to provide an essentially constant rms mains voltage during these experiments.

In order to reduce the number of variables, the peak open-circuit voltage of each generator was adjusted to approximately 1 kV. The amplitude control on the front panel of the generator was not adjusted during the remaining experiments with that waveform.

### Does the actual waveform satisfy the specifications ?

The parameters for each experimental waveform (front time, duration, etc.) were determined and compared with the nominal values in the relevant specification. In this manner, an objective assessment can be made on the adequacy of the waveforms in meeting the requirements of the standards.

Because the data taken from the digital oscilloscopes is quantized, the data contain random fluctuations of one or two least significant bits in addition to small oscillations that may be part of the actual waveform. To suppress errors caused by these fluctuations and oscillations, a limited amount of processing was done to obtain the peak value, the 10% (or 30%) and 90% points on the leading edge of the waveform, and the 50% point on the tail of the waveform. The details of this processing are specified in Appendix II.

Table 1 gives the measured front time and duration of the 1.2/50 μs and 8/20 μs waveforms. No duration is available for the 1.2/50 μs waveform from generator C because of an oversight by the author. Fig. 3 shows the open-circuit voltage waveform; Fig. 4 shows the short-circuit current waveform. In order to have a meaningful comparison of the waveshapes each set of data was normalized to

Table 1
Measured Waveshape Parameters

| Generator | measured front/duration μs | | discrepancy from nominal front | duration |
|---|---|---|---|---|
| *open-circuit voltage* | | | | |
| A | 1.21 | 57.43 | 0.8% | 15% |
| B | 1.57 | 55.2 | 31 % | 10% |
| C | 1.22 | | 1.7% | |
| *short-circuit current* | | | | |
| A | 9.24 | 26.70 | 16% | 34% |
| B | 8.56 | 25.72 | 7% | 29% |
| C | 10.86 | 28.50 | 36% | 42% |
| D | 8.34 | 24.28 | 4% | 21% |

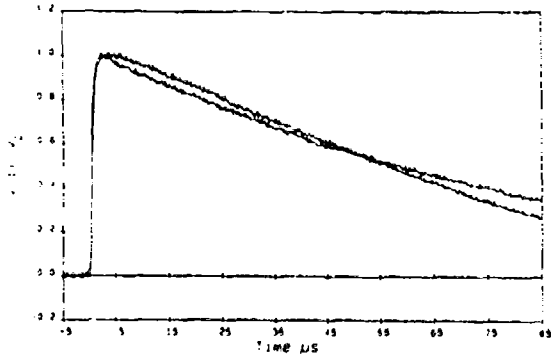


Fig. 3 Open-circuit voltage waveforms from generators A and B. The actual peak values were 867 and 952 V.

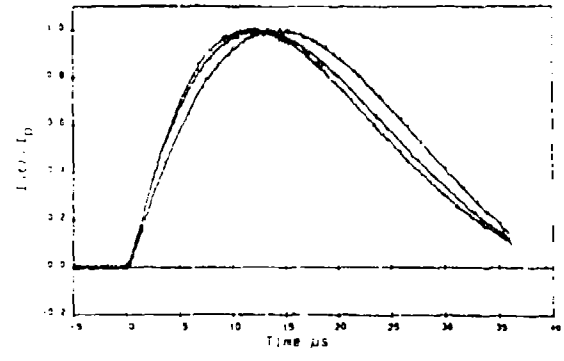


Fig. 4 Short-circuit current waveforms from generators A, B, and C. The peak currents were 392, 606, and 555 A.

have a peak value of 1.0 and an offset was added to time in each set of data to make the virtual origin occur at t = 0.

Note that all of the measured durations are significantly longer than the nominal value. All of the generators met, or nearly met, the specifications for the 1.2/50 μs waveform. None of the generators satisfy the specifications for the duration of the 8/20 μs waveform; moreover half of the generators do not satisfy the specification for front time.

Ring wave The measured parameters for the ring wave are given in Table 2. The definition of the ring wave in [3] gives specifications only for the voltage waveform, although Table 2 also gives parameters for the current waveform. The open-circuit voltage waveforms for all three generators is shown in Fig. 5. The value of the initial peak was normalized to 1.0. So that the variations in frequency could be clearly seen, an offset was added to time in Fig. 5 to make all of the waveforms have a first zero-crossing after the initial peak at t=0. Notice in Fig. 5 that the waveshape of the first peak is remarkably different for each of the three generators. The waveform from generator A has several reversals in slope during the first cycle.

There are three amplitude ratios given in Table 2. The value in the left column is the ratio of the amplitude of the first two peaks, the value in the middle column is the ratio for the second and third peak, and the value in the right column is the ratio of the third and fourth peaks. Notice that the amplitude ratio changes significantly between half-cycles for some of the generators. Part of the reason for this is that the specification for the waveform can *not* be satisfied by a cosine waveform with an exponentially decaying amplitude [9].

Martzloff [5] discussed properties of two different surge generators for the 100 kHz ring wave that gave essentially the same open-circuit voltage waveform but different short-circuit current waveforms. Such a result is easy to understand. Common surge generators have a pulse-shaping network that is composed of resistors, capacitors, and inductors. There are different networks that will provide the same open-circuit voltage waveform. However, when a short-circuit is applied across the output terminals, one would expect different output current waveforms because different components in the pulse-shaping network are shorted.

Effective Impedance

In an attempt to make the behavior of surge generators more reproducible when used with different loads, Martzloff [6] used the concept of "effective impedance," the ratio of peak open-circuit voltage to peak short-

Table 2
Measured Waveshape Parameters for 100 kHz Ringwave

| Generator | measured rise time µs | measured ratio of peaks % | measured frequency kHz | discrepancy from nominal rise time | discrepancy from nominal ratio of peaks % | discrepancy from nominal freq. % |
|---|---|---|---|---|---|---|
| *open-circuit voltage* | | | | | | |
| P | 0.38 | 51 67 65 | 103.5 | -24% | -15 12 08 | 3.5 |
| Q | 0.39 | 66 69 70 | 76.5 | -22% | 10 15 17 | -23.5 |
| R | 0.63 | 73 72 49 | 94.6 | +26% | 22 20-18 | -5.4 |
| *short-circuit current* | | | | | | |
| P | 0.85 | 56 52 53 | 164 | not specified | | |
| Q | 0.90 | 88 30 39 | 83 | | | |
| R | 0.77 | 66 47 | 87 | | | |

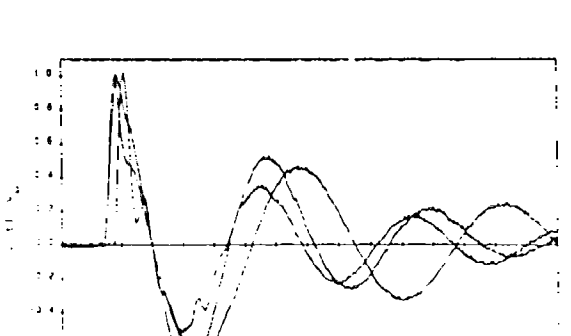


Fig. 5 Open-circuit voltage waveforms from generators P, Q, and R. The peak voltages were 981, 934, and 980 V.

circuit current. Because the open-circuit voltage and short-circuit current have their peaks at different times, the effective impedance is *not* the Thévenin impedance of the surge generator. While Martzloff admitted that effective impedance was not a rigorous parameter, it is easy to determine and convenient.

Table 3 shows the effective impedance values for six generators in this study. The specifications give no tolerance for this important parameter.

other considerations

Some surge generators have one output terminal connected to earth. This is acceptable for testing of components, but presents difficulties when the surge generator is to be coupled to nongrounded conductors for testing vulnerability of electronic equipment.

Often surge generators are connected to test equipment that is powered from the ac supply mains. In order to inject a high-voltage surge on the mains, a "back-filter" must be inserted between the supply and the generator so that nearly all of the surge current goes into the equipment under test. Conventional back filters consist of a series inductor and capacitors shunted across the line on the mains side of the filter. The series inductor presents a smaller impedance to lower frequencies components of the surge waveform, so that the back filter will modify the surge waveform. Richman [7] has suggested that the back filter be considered part of the surge generator, so that the generator will give the proper waveshape when the back filter is connected. Tests of the effects of back filters on waveforms was beyond the scope of the research reported here.

Part II: What is the effect of other loads ?

Specifications for overvoltage test waveforms are given for idealized loads: voltage waveforms are specified for an open-circuit load, current waveforms are specified for a short-circuit load. When a voltage waveform is used to test insulation, the actual load approximates an open-circuit. When a current waveform is used to test a device with a small resistance, V/I, the

Table 3
Effective Impedance of Generators:
open-circuit voltage/short-circuit current

| Generator | Measured Value | Nominal Value | Discrepancy |
|---|---|---|---|
| *combination 1.2/50 and 8/20 µs* | | | |
| A | 2.22 Ω | 2 Ω | +11% |
| B | 1.56 Ω | 2 Ω | -22% |
| C | 1.73 Ω | 2 Ω | -14% |
| *100 kHz ring wave* | | | |
| P | 13.2 Ω | 12 Ω | +10% |
| Q | 35.0 Ω | 30 Ω | +17% |
| R | 10.3 Ω | 12 Ω | -14% |

actual load approximates a short-circuit. But for other types of tests, the actual load may be far from the idealized open-circuit or short-circuit.

To evaluate the effects of different loads on the waveform, the output voltage and current of each generator was measured for each of the following conditions:

1. open-circuit,
2. short-circuit,
3. metal-oxide varistor (MOV) rated for service on 130 V rms mains,
4. metal-oxide varistor (MOV) rated for service on 320 V rms mains, and
5. 0.1 μF capacitor.

The two varistors are typical of devices that are used to protect equipment from overvoltages on the mains. The 130 V model has the lowest conduction voltage of any model suitable for connection to mains with a nominal voltage of 120 V rms. The 320 V model has an appreciable safety margin for connection to mains with a nominal voltage of 250 V rms. The specific models of the varistors used in the experiments were General Electric V130HE150 and General Electric V320PA40A.

The capacitor is typical of those in low-pass filters for connection to the ac supply mains: it had a metallized polyester dielectric which is self-healing after breakdown. The specific model used in the experiments had a dc voltage rating of 6 kV. A resistance of 6.8 MΩ was permanently connected in shunt with the capacitor for safety reasons.

The results of this part of the experiment are summarized in Table 4 for the combination waveform and in Table 5 for the 100 kHz ring wave. A plot of the normalized voltage across a varistor from two combination waveform generators is shown in Fig. 6.

When a voltage waveform is applied across a short-circuit or a load with a small value of V/I, the current is determined by the output impedance of the generator as well as the voltage waveform. When a current waveform is applied across an open-circuit or a load with a large value of V/I, the voltage across the load is determined by the voltage on the energy storage capacitor inside the generator, as well as by details of the wave shaping circuit inside the generator.

Table 4
Effect of Various Loads on Waveshape

*voltage waveforms:* front/duration μs

| generator | no load | 130 V MOV | 320 V MOV | 0.1 μF capacitor |
|---|---|---|---|---|
| A | 1.21/57.4 | 0.70/44.5 | 0.77/61.5 | 2.46/5.13 |
| B | 1.57/55.2 | 0.67/30.9 | 1.05 | 2.47/5.21 |
| C | 1.22 | 0.38 | 0.65 | 2.43/5.24 |

*current waveforms:* front/duration μs

| generator | short | 130 V MOV | 320 V MOV | 0.1 μF capacitor |
|---|---|---|---|---|
| A | 9.24/26.7 | 6.54/25.3 | 5.41/16.6 | 1.38/2.90 |
| B | 8.56/25.7 | 7.99/21.6 | 6.60/18.8 | 1.58/3.02 |
| C | 10.86/28.5 | 10.28/27.2 | 7.57/20.8 | 1.26/2.78 |
| D | 8.34/24.3 | 7.70/20.7 | 5.70/12.9 | 1.14/2.45 |

Table 5
Effect of Various Loads on 100 kHz Ringwave *Voltage* Waveform

| generator | no load | 130 V MOV | 320 V MOV | 0.1 μF capacitor |
|---|---|---|---|---|
| *risetime (μs)* | | | | |
| P | 0.38 | 0.23 | 0.29 | 1.09 |
| Q | 0.39 | 0.28 | 0.34 | 0.80 |
| R | 0.63 | 0.37 | 0.51 | 1.27 |
| *rate of decay of first two peaks (%)* | | | | |
| P | 51 | 88 | 58 | 83 |
| Q | 66 | 96 | 77 | 55 |
| R | 73 | 98 | 86 | 87 |
| *frequency (kHz)* | | | | |
| P | 103.5 | 102 | 103 | 82 |
| Q | 76.5 | 77 | 77 | 62 |
| R | 94.6 | 95 | 94 | 87 |

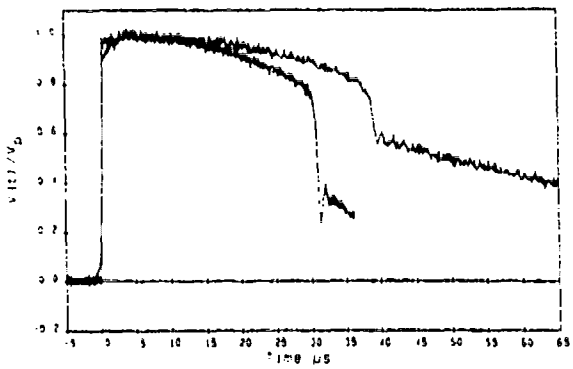

Fig. 6 Voltage waveforms from generators A and B measured across a metal oxide varistor rated for service on mains with a nominal voltage of 130 Vrms.

The clamping action of the varistor makes the voltage essentially constant when there is an appreciable current in the varistor (compare Figs. 3 and 6). For example, the peak open-circuit voltage of generator B was 952 V, while the peak voltage across the 130 V rms rated MOV was only 317 V. This clamping action of the varistor makes the ratio of successive peaks of the ring wave be larger than the specified 60%, as shown in Table 5.

When the capacitive load is connected, the rise time for voltage is increased for all waveforms. This would be expected since the output resistance of the generator and the capacitance of the load forms a low-pass filter. The capacitive load decreases the oscillation frequency of the ring wave, as would be expected.

PART III: More comprehensive specifications

The decision on whether or not a unipolar waveform is satisfactory is determined after considering the value of the waveform at only three different points, as shown in Fig. 7. The author believes that such specifications are incomplete. The waveform should also approximate an ideal waveshape and be smooth (no large discontinuities, no large undesired oscillations). These are not new considerations. McAuley and Benedict stated

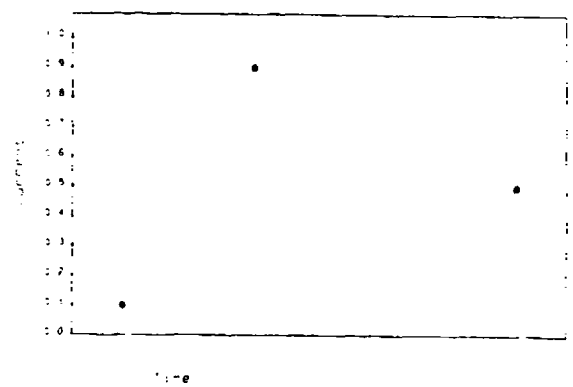

Fig. 7 The traditional specification of a unipolar waveform uses three points on the waveform. Compare with Figs. 1 and 9.

them concisely 55 years ago:"...the present wave definitions are not exact. Only the time to crest and time to half-value of the wave are specified. Hence it is possible to conform to these conditions and at the same time have a wave so distorted with oscillations, that reasonably accurate and comparable voltage measurements [with sphere gaps] are impossible. The spirit of the definition assumes that the wave follows exponential curves."[8] Simple mathematical relations have been given for the most common high voltage test waveforms [9]. One goal of this paper is to suggest ways for a more comprehensive specification for high voltage test waveforms, by comparing actual waveforms to the "ideal" waveform given by the mathematical relation.

Before waveforms from surge generators can be compared to an "ideal equation," one must find the ideal. Many engineers [8,10,11] have stated that the ideal waveshape for most unipolar voltage waveforms is specified by a double exponential relationship, Eqn. 4

$$V(t) = A\,V_p\,(\,1 - \exp(-t/\tau_1)\,)\,\exp(-t/\tau_2) \qquad (4)$$

Eqn. 4 represents the solution for the output voltage of common RC pulse-shaping networks used in surge generators, so there can be no doubt that this is the ideal relationship.

If the double exponential relation and the nominal values of parameters A, $\tau_1$, and $\tau_2$ were accepted as the ideal waveform, then one might evaluate surge generators by fitting the actual waveform to the ideal equations (e.g., by the method of least-squares) and examining the resulting values of the parameters. Tolerances would be specified for the parameters in the double exponential relation, rather than the present practice of specifying tolerances on the front time and duration. Fitting the actual waveform to the ideal equation and examining the resulting parameters would have the advantage that the entire waveform is considered, and not just the value of the waveform at three different points. However, if the actual waveform has a much different shape than the ideal waveform, the resulting set of parameters is *meaningless* (although the values might be within acceptable limits). If the actual waveform has a shape that is very near the ideal, then the present criteria for examining just three points is adequate and there is no need for complicated curve-fitting to a set of experimental data. Therefore, fitting the actual waveform to an ideal equation is not a desirable qualification test for the waveform.

proposal for acceptable waveform

A more comprehensive specification would be to construct boundaries for variations in a test waveform so that tolerances apply over most of the waveform, and not just at several points. This effort can be done in either the time or frequency domain (1) by specifying a region in the t, V(t) plane, or (2) by evaluating the Fourier transforms of the waveform and the equation for the nominal value of V(t), and then specifying a region in the $\omega$, $V(\omega)$ plane. Examples of proposed

tolerances for the time domain are given for the 1.2/50 and 8/20 μs waveforms.

Construction of upper and lower bound curves in the time domain is simple. The upper bound has the minimum front time, the maximum peak value, and the maximum duration. The lower bound has the maximum front time, the minimum peak value, and the minimum duration. For the 1.2/50 and 8/20 μs waveforms, the tolerances in [1,2] have been used to establish these maximum and minimum values.

proposed tolerances on the 1.2/50 μs waveform

The 1.2/50 μs waveform is used as an example of how to construct an upper and lower bound for an acceptable double exponential waveform in the time domain. As the upper and bound curves have a different virtual origin from the nominal curve, it is desirable to use a change of variable $t' = t + t_o$ in Eqn. 4. All three curves have the same virtual origin when the translated time, t', is used. The values of the parameters for Eqn. 4 for each of the three curves are:

| | $\tau_1$ μs | $\tau_2$ μs | A | $t_o$ μs |
|---|---|---|---|---|
| upper | 0.2755 | 83.67 | 1.053 | -0.156 |
| nominal | 0.4075 | 68.22 | 1.037 | -0.220 |
| lower | 0.5558 | 52.84 | 1.028 | -0.282 |

When using these parameters with Eqn. 4, $V_p$ is the nominal peak voltage: the value of $V_p$ needs no adjustment since the tolerances on the peak are contained in the values for A for the upper and lower bound curves. Fig. 8 shows plots of the lower bound, nominal, and upper bound curves.

An actual waveform could go outside of these boundaries for any of several different reasons. The actual waveform might be double-exponential, but have an unacceptable value of one or both time constants. The actual waveform might be the superposition of a double-exponential with relatively large oscillations. Or the actual waveshape may be far from a simple double-exponential waveform, perhaps due to large discontinuities.

References [1,2] give a tolerance of ±3% for measurements of the peak voltage of a 1.2/50 μs waveform. This appears to be a very strict specification. The vertical amplifiers in commonly used analog oscilloscopes have an accuracy of ±2% when calibrated to the manufacturer's specifications. There is additional error, which is often on the order of ±3%, in the attenuation of commonly used high-voltage probes. It appears that the measurement error will usually be larger than the ±3% tolerance between indicated and nominal value. It may be appropriate to change the tolerance on the peak value to, for example, ±10%.

proposed tolerances on the 8/20 μs waveform

There is no double exponential representation for the 8/20 μs waveform, however [9] showed that Eqn. 5

$$I = A\, I_p\, t^k \exp(-t/\tau) \qquad (5)$$

was a simple relation for the 8/20 μs waveform. Because the upper and lower bound curves have different virtual origins from the nominal curve, it is desirable to use the translated time, t', where $t' = t + t_o$. The parameters for Eqn. 5 that yield the three curves are:

| | k | τ μs | $A\ (\mu s)^{-k}$ | $t_o$ μs |
|---|---|---|---|---|
| upper bound | 1.5779 | 6.2538 | 1.4384E-01 | 0.21 |
| nominal | 3.00 | 3.9114 | 1.2431E-02 | 1.67 |
| lower bound | 9.21 | 1.8759 | 3.6058E-08 | 6.87 |

Fig. 9 shows a plot of all three curves. It is proposed to begin to apply the upper and lower bound curves at the 30% point on the leading edge of the waveform, as shown in Fig. 9. For earlier times, the upper and lower bound curves approach the nominal curve too closely.

As reported in Part I of this paper, commercial surge generators do not meet the present ±10% tolerance on duration or front time. Because there is no evidence that these commercial surge generators are unsatisfactory in actual practice, the tolerances on the front time and duration should be changed, from the present value of ±10% to perhaps -10,+30%.

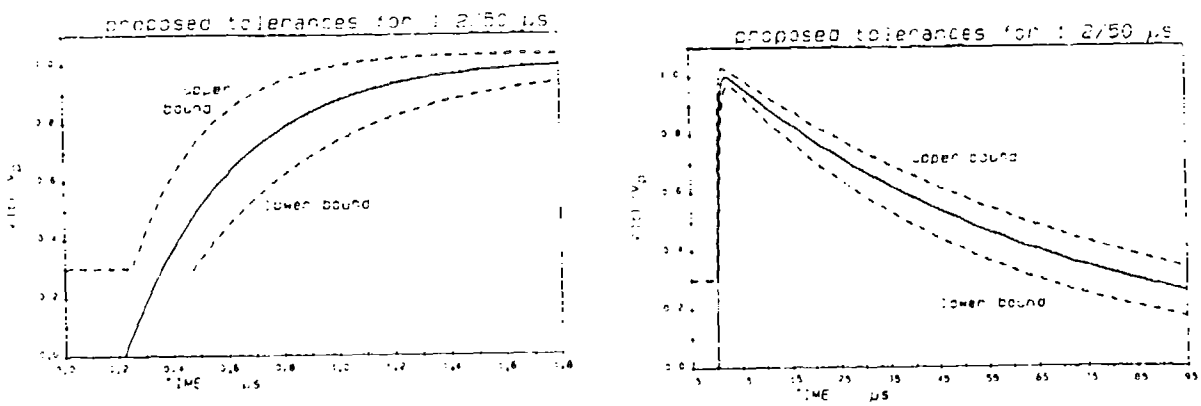


Fig. 8 Proposed specification for a 1.2/50 μs voltage waveform. Any waveform that is between the two dashed lines is acceptable. The nominal waveform is shown as a solid line.

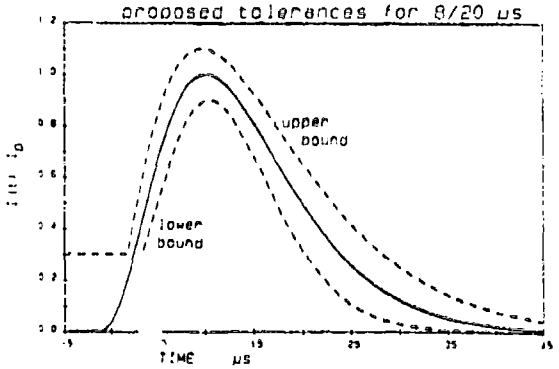


Fig. 9 Proposed specification for an 8/20 μs current waveform. Any waveform that is between the two dashed lines is acceptable. The nominal waveform is shown as a solid line.

With this increase in tolerance, it may also be desirable to specify the total charge transfer, $\Delta Q = \int I\,dt$, during short-circuit loading of the generator. Many practical surge protective devices (e.g., varistors and avalanche diodes) have an essentially constant voltage during passage of appreciable surge currents. The energy, which is an important parameter, that is transferred to devices with a constant voltage is proportional to $\Delta Q$. For example, one might require

$$\Delta Q = (17.5\ ^{+5.4}_{-4.5}\ \mu s)\ I_p$$

These tolerances on $\Delta Q$ agree with the proposed upper and lower bound curves given above. The nominal value of $\Delta Q$ corresponds to the nominal current from Eqn. 5.

long-duration unipolar waveforms

There are several special considerations for specifications for unipolar long duration waveforms, such as the 10/700 μs and 10/1000 μs waveforms. Such long duration waveforms, when provided by a surge generator with a small output resistance, can transfer large energy to a load. If the ideal waveshape is a double exponential, the energy transferred depends on the values of the peak open-circuit voltage, $V_p$, and the decay time constant, $\tau_2$. The value of the time constant for the leading edge of the waveform, $\tau_1$, has a trivial effect on the energy content of the waveform because the time from the origin to the peak of the wave is much smaller than the duration of the waveform. Therefore, one might wish to place small tolerances (e.g., ±5%) on the peak value, $V_p$, and the decay time constant, $\tau_2$, and relatively large tolerances (e.g., ±30%) on the value of the time constant for the leading edge, $\tau_1$.

oscillatory waveforms

It is especially complicated to construct boundaries in the time domain for an oscillatory waveform. If the frequency of oscillation alone is allowed to vary then the various boundaries for an acceptable ring waveform overlap at time increases. Boundaries for oscillatory waveforms may be simpler when viewed in the frequency domain than in the time domain. It is common to view frequency domain data as a plot with logarithmic scales for both amplitude and frequency. The effect of logarithmic scales is to compress small discrepancies, which is a disadvantage in setting specifications. Many laboratories still use analog oscilloscopes to measure high-voltage surges. Until digitizing oscilloscopes interfaced to computers with digital signal processing software become common, it is premature to specify high-voltage test waveforms in the frequency domain.

## Acknowledgments

An evaluation of commercial surge generators was suggested by F.D. Martzloff as part of the work supporting the present revision of ANSI C62.41. This research (including the purchase of all equipment) was supported by a contract with Allegheny Power System; thanks are due to W.C. Guyker, Jr. for recognizing the importance of developing engineering standards. Additional funding was provided by the U.S. Army Research Office. Evaluations of commercially available generators would not have been possible without the generous cooperation of KeyTek Instrument Corp., Velonex, and Haefely. M. Hopkins and B. Cormier of KeyTek witnessed the testing of their products. I also wish to thank D. Shakarjian for constructing and testing the custom trigger circuits that were used in the measurements and for witnessing all of the measurements.

## References

[1] IEC 60-2, "High-Voltage Test Techniques, Part 2: Test Procedures" (1973)

[2] IEEE Standard 4, "IEEE Standard Techniques for High-Voltage Testing" (1978)

[3] ANSI C62.41, "IEEE Guide for Surge Voltages in Low-Voltage AC Power Circuits" (1980)

[4] Standler, R.B., Protection of Electronic Circuits from Overvoltages, Wiley-Interscience, New York (1989)

[5] Martzloff, F.D., "Transient Control Level Test Generators," General Electric Corporate Research and Development Technical Report 77CRD241 (1977)

[6] Martzloff, F.D., "The Propagation and Attenuation of Surge Voltages and Surge Currents in Low-Voltage AC Circuits," IEEE Trans. Power Apparatus and Systems, 102:1163-1170, (1983)

[7] Richman, P., "Changes to Classic Surge Test Waves Required by Back Filters Used for Testing Powered Equipment," Proc. 6th EMC Symposium Zürich, pp. 413-418, (1985)

[8] McAuley, P.H. and F.R. Benedict, "Calculating Surge Generator Waves," The Electric Journal, 30:326-328, (1933)

[9] Standler, R.B., "Equations for Some Transient Overvoltage Test Waveforms," IEEE Trans. Electromagnetic Compatibility, 30:69-71, (1988)

[10] Allibone, T.E., and F.R. Perry, "Standardization of Impulse-Voltage Testing," IEE Journal, 78:257-272, (1936)

[11] Hylten-Cavallius, N., "Comments on 'Definition of Switching Surge Waveshapes' by H.M. Smith, et al.", IEEE Trans. Power Apparatus and Systems, 86:1407, (1967)

## Appendix I: Instrumentation

The Tektronix 2430 oscilloscopes that were used in these experiments digitize the signals with a dynamic range of 256 states ($2^8$ bits) and take 1024 samples of each signal per record. The oscilloscopes are interfaced to a digital computer which collects the data, reads the scale factors from the oscilloscope, determines the zero levels, and stores the data on a magnetic disk. Immediately after each waveform is acquired, the computer connects all four oscilloscope inputs to earth, waits 2 seconds, and digitizes a blank record. All 1024 points in each channel are averaged to obtain an accurate zero reference level, which is subtracted from the data before processing.

Tektronix P6009 probes were used to measure the voltages between each side of the load and earth, $V_{HG}$ and $V_{NG}$. The 120 MHz bandwidth of the probes was not a limitation during these experiments, since at the maximum sample rate the data bandwidth is only 40 MHz. These probes were compensated in the usual way, then the compensation of the NG probe was adjusted slightly to maximize the common-mode rejection ratio, as described in [4]. All of the voltage data shown in this paper is the difference, $V_{HN}$, between the two measured voltages.

The surge currents were measured with Ion Physics Corp. model CM-10-L current transformers with a sensitivity of 10 A/V. This sensitivity was reduced by using a 50 Ω coaxial resistive 20 dB attenuator near the inputs of the oscilloscope. The manufacturer states that the 3 dB bandwidth of the current transformers extends from 5 Hz to 40 MHz, and that the core of the current transformer will not saturate for values of $\int I\,dt$ less than 1 kA·100 μs. This experiment did not require two independent measurements of current, $I_H$ and $I_N$. However since they were available, all of the data shown in this paper is the average of two independent measurements, $(I_H - I_N)/2$. This average reduces the random noise in the digitization process.

The two voltages, $V_{HG}$ and $V_{NG}$, were measured simultaneously on one oscilloscope. The two currents, $I_H$ and $I_N$, were measured simultaneously on the other oscilloscope. Both oscilloscopes had the same nominal sample rate and were triggered from the same external trigger source.

Both voltage and current were measured during all tests, even during Part I. Because the peak voltage was negligibly small (<15 V) when the load was a short-circuit, we can be certain that the magnetic field from surge currents as large as 610 A had negligible effect on the measurement of voltage. Similarly, the fact that the peak current was negligibly small (<1.0 A) when the load was an open-circuit shows that the electric field had negligible coupling to the output of the current transformer. Such checks are desirable because electromagnetic fields can couple erroneous signals, for example, into the loop area between voltage probes.

## Appendix II
## Processing of data to determine front time and duration

A computer program was written to automatically process the data and determine the front time and duration for each waveform. The data are arranged in an array of coordinate pairs $(t, V_{HN})_i$, where i is the integer index.

### peak value of unipolar waveforms

The front time and duration are defined in terms of the peak value, $V_p$, so the first task is to determine the best estimate of the peak value. The program scans all of the samples starting with the earliest (i=1) and ending with the latest (i=1024). The program finds the largest value of $|V_{HN}|$ in each data file, which occurred at the $j^{th}$ sample. If the same maximum value occurred at two or more samples in one data file, the earliest occurrence was used for the value of j. The peak voltage, $V_p$, was then calculated from the average value of the five samples between j-1 and j+3. More points were taken after the largest value of $|V_{HN}|$ than before because the decay of the overstress waveform is less rapid than the initial rise.

### front time of unipolar voltage waveforms

Once $V_p$ has been determined, the times of occurrence of the 30% and 90% points on the leading edge are found. The program scans the data starting with the earliest (i=1) sample until the first occurrence of a voltage $V_{HN} \geq (0.3\ V_p)$ is found at the $k^{th}$ sample. The program then fits a straight line by the method of least-squares through the seven coordinate pairs starting at sample k-2 and ending at sample k+4, which gives a line of the form:

$$V_{HN}(t) = a\,t + b$$

The assumption is made in the least-squares routine that the time of each sample is exact and that only the voltage values have errors. This assumption is justified because the quartz crystal timebase in the oscilloscope is much more accurate than the voltage digitization. The time of the 30% point, $t_1$, is found by

$$t_1 = [(0.3\ V_p) - b]/a$$

The least-square linear curve fitting and interpolation is used to accurately specify

the time $t_1$ even when the data have oscillations and random fluctuations (noise).

A similar process is used to find the time of the 90% point on the leading edge, $t_2$, and the time of the 50% point on the tail of the waveform, $t_3$.

These algorithms give identical values of front time to 3 significant digits for the 1.2/50 μs waveform from one model of surge generator when the voltage data are sampled at intervals of either 0.01 μs or 0.10 μs. This shows that processing of the data can be used to increase the effective resolution of the data.

unipolar current waveforms

The current waveforms were processed in the same way, except that the 10% point instead of the 30% point on the leading edge is used to calculate the front time.

parameters for ring waveform

The largest value of $|V_{HN}|$ in the record is found in the same way as the peak of the unipolar voltage waveform, except that only four samples are averaged. The value of the first peak is called $V_p(0)$.

The zero-crossings of the waveform are found next. The program searches for the first zero crossing *after the largest peak*, when

$$(V_{HN})_j * (V_{HN})_{j+1} \leq 0$$

The program then fits a straight line through the data between the j-2 and j+4 samples, including the end points. The time of the zero of this straight line is called $t_z(1)$, which is the best estimate of the time of the first zero-crossing.

The program resumes the search for the next zero at sample

$$j + \text{INT}(2.5\ \mu s/\Delta t)$$

where j is the integer sample number nearest the previous zero, 2.5 μs is one-quarter of the nominal period of oscillation, and Δt is the time between successive samples. The next five zeroes are found in the same way as the first and called $t_z(2), \ldots, t_z(6)$.

The average frequency of oscillation, $\bar{f}$, is determined from the first five zeroes after the largest peak:

$$\bar{f} = 2/[t_z(5) - t_z(1)]$$

The program then finds the values of the other peaks, $V_p(i)$, by searching for the largest value of $|V_{HN}|$, which occurs at the $j^{th}$ sample, between two successive zero-crossings, $t_z(i)$ and $t_z(i+1)$, where $1 \leq i \leq 5$. The value of each peak is obtained by an average over four points from the j-1 to the j+2 sample.

The rise time of the leading edge of the ring waveform is found last. The values of the 10% and 90% points for the rise time are found in the same way as for unipolar waveforms.

May 1988 pp. 66-73

# Use of Low-Pass Filters to Protect Equipment from Transient Overvoltages on the Mains

RONALD B. STANDLER
SENIOR MEMBER, IEEE
Communications and Space Sciences Laboratory
Department of Electrical Engineering
The Pennsylvania State University
University Park, PA 16802

Abstract - The design of commercial low-pass filter modules for equipment connected to the low-voltage supply mains is reviewed. Problems of using these filters to protect electronic equipment from damage or upset by high-voltage transients on the mains are discussed. The design and performance of circuits that incorporate both overvoltage protection and a low-pass filter are discussed. One circuit is designed for commercial environments, the other for medical equipment in patient care areas. Filters for medical equipment in patient care areas must have very small line-to-ground leakage currents, which makes it difficult to provide either overvoltage protection or low-pass filtering. Using an overvoltage-protected low-pass filter is less expensive than using a line conditioner to protect equipment, and, in many instances, the filter may give satisfactory protection.

## I. INTRODUCTION

Low-pass filters are commonly connected in series with the power cord for electronic equipment to achieve electromagnetic compatibility. These filters attenuate high frequency noise that is generated inside the chassis and conducted on the power cord out of the chassis and into the environment. This application of filters is well known and covered in many standards and regulations. Low-pass filters may also protect equipment from some disturbances on the mains, such as high-frequency noise and transient overvoltages.

High-voltage transients on the mains can damage electronic circuits or cause temporary malfunction (upset) of these circuits. Common sources of high-voltage transients include lightning strikes to overhead power lines and switching of reactive loads [1]. Transient overvoltages with a peak value greater than about 500 V are rare events. Bursts of high-frequency noise with a peak-to-peak value between 90 and 100 V occurred at one residential site at an average rate of 0.5 per hour [2]. Maximum values of $|dV/dt|$ of the order of 1 kV/μs were common. Because the peak voltage values in these bursts of noise are less than the amplitude of the steady-state mains voltage, overvoltage protection (e.g., metal oxide varistors) will be ineffective in attenuating these disturbances. However, a low-pass filter could be effective in attenuating these bursts of noise. This paper examines the design and use of low-pass filters to protect equipment from high-voltage transients on the mains.

High-frequency noise is transferred from the mains through step-down transformers by parasitic capacitance between the primary and secondary coils [3]. Therefore, the high-frequency noise at the secondary may be larger than would be expected on the basis of the turns ratio and the amplitude of the noise on the mains. One cannot rely on common dc voltage regulator circuits to attenuate high-frequency noise or transient overvoltages because these circuits do not reject high-frequency noise at the same degree as the ripple voltage at twice the mains frequency on account of limitations imposed by the gain-bandwidth product. Electrolytic filter capacitors that reduce the ripple in dc power supplies have appreciable series inductance which makes them ineffective for bypassing noise to ground at frequencies of about 1 MHz or greater. Therefore, high-frequency noise or transient overvoltages on the mains may be able to propagate through a dc power supply and upset the operation of an electronic circuit.

Common low-pass filter modules for commercial service provide approximately 30 dB to 70 dB of attenuation in a 50 Ω system at frequencies between 0.15 MHz and 30 MHz. Owing to limitations on the physical size of inductors and capacitors, most filters have little attenuation at frequencies below [illegible] MHz. However, mains filters for switching power supplies may need significant attenuation at frequencies as low as 10 kHz. Common transient overvoltages have appreciable energy at frequencies below 1 kHz. Above about 30 MHz most noise is transferred in or out of a chassis by radiation through space rather than by conduction along wires.

A transient on the mains with a peak value of 2000 V would be attenuated to about 60 V by a filter with an attenuation of 30 dB. This amount of attenuation might be adequate. However, a problem arises because a filter that is rated to have an attenuation of 30 dB may have less attenuation during high-voltage transients. Filters are normally characterized with a sinusoidal voltage with an amplitude of only a few volts. Attenuation data from these experiments are not relevant to performance during high-voltage transients for the following reasons:

(1) The dielectric in shunt capacitors may break down and produce a large value of dV/dt inside the filter, which behaves as an unexpected source.
(2) The inductance of chokes typically decreases during large currents owing to partial or complete saturation of ferromagnetic core material. Abnormally large currents may flow in chokes during high-voltage transients.
(3) Large voltage stresses across series inductors may cause insulation breakdown and shunt the inductor with an arc.
(4) Attenuation data in manufacturer's specifications is measured with a 50 Ω resistive load. While this is a reproducible test method, it does not correspond to actual operating conditions [4].

The last reason is particularly insidious. The 50 Ω resistive load in the standard test method damps resonances that may be present with the LC elements in the filter. Furthermore, a reactive load during real-world operation of the filter may cause resonance with the output port of a low-pass filter and produce voltage gain [5].

## II. CONVENTIONAL DESIGN OF FILTERS

Modern, low-cost filter modules for commercial service have a typical circuit configuration shown in Fig. 1.

The inductor in Fig. 1 has two identical coils that are wound on a ferrite toroid, as described by

CH2581-7/88/0000-0066 $1.00 ©1988 IEEE

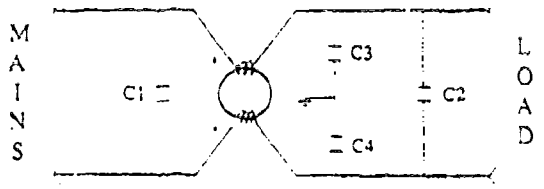


Fig. 1. Typical low-cost, low-pass filter module for use between mains and electronic equipment.

[6]. This component is called a "common-mode choke," since it presents a much larger inductance to common-mode than to differential-mode signals. A typical common-mode choke in a mains filter has an inductance between about 1 mH and 30 mH to common-mode signals. The inductance for differential-mode signals is of the order of 30 μH [7]. The small differential-mode inductance prevents saturation of the magnetic core by normal load currents, which may be of the order of 1 to 20 A rms. For this reason, this component is sometimes called a "current-compensated choke." The continuous toroidal core structure is particularly desirable because it has no air gap to radiate magnetic field and increase ambient electromagnetic noise levels.

There are two practical ways to connect capacitors in a low-pass filter for the mains. One or more capacitors, such as C1 and C2 in Fig. 1, can be shunted between the hot and neutral conductors to attenuate differential-mode noise. Or a pair of capacitors, such as C3 and C4 in Fig. 1, can be shunted between ground and each mains conductor to attenuate common-mode noise. The capacitance values of C3 and C4 are nominally identical, so that common-mode noise is not converted to appreciable differential-mode noise by unbalanced impedances. The capacitance of either C1 or C2 is usually between about 0.1 μF and 0.5 μF, and it can be made larger. The capacitances of C3 and C4 must be small for safety reasons; values of the order of 2 nF are typical. If the ground connection were open, an electric shock hazard would exist if the capacitance between the hot conductor in the mains and the chassis ground is large.

The maximum capacitance between the mains and ground is determined by the allowable leakage current. The leakage current is measured between the conducting case (which must normally be connected to circuit ground) and the mains neutral conductor when the filter is connected to the mains without a ground wire. The maximum leakage current, and the maximum capacitance for use on 120 V rms, 60 Hz mains, is given in Table 1.

The input capacitor, C1 in Fig. 1, is vulnerable to damage by transient overvoltages on the mains. Consider the common 8/20 μs current waveform with a peak of 500 A that is used for testing surge protective devices. This test waveform transfers 6.7 mC of charge. If we consider a typical π filter with two 0.5 μF capacitors and a 30 μH choke, the potential difference across the capacitors will have a peak value of about 9.6 kV. This large voltage across the capacitor could cause dielectric breakdown, followed by an arc inside the capacitor. The peak voltage of 9.6 kV that is predicted by calculation would probably not occur in a realistic situation: common electrical outlets flashover at a potential of about 6 kV. Whatever the peak voltage may be during a severe overstress, it still threatens the dielectric in shunt capacitors.

Table 1
Maximum Leakage Current and Capacitance

| environment | maximum rms leakage current | maximum capacitance line to ground 120 V rms 60 Hz service |
|---|---|---|
| medical equipment: patient care area | 0.1 mA | 2.2 nF |
| residential and non-patient care medical | 0.5 mA | 11 nF |
| commercial | 3.5 mA | 77 nF |

Maximum leakage current specifications are contained in section 27 of Underwriters Laboratory Standard 544 (for medical equipment) and in section 24 of Underwriters Standard 1283 (for mains filters).

To avoid destruction of unprotected filters during operation when connected to the mains, specifications commonly address behavior during transient high-voltage stresses. For example, [8] requires filters that are rated for 250 V ac or less to withstand a potential difference of 1414 V dc between the hot and neutral terminals and a potential difference of 2121 V dc between ground and either the hot or neutral conductor.

An additional problem with filters during transients is the possible resonance that may cause the amplitude of the voltage across the output port to exceed the amplitude of the source voltage. There are several techniques to avoid constructing a high-Q resonant circuit. Chokes with a ferrite core can be fabricated to have a large resistive component of impedance at frequencies between about 0.1 MHz and 10 MHz. This resistance damps oscillations in an otherwise pure LC circuit without using resistors. The permeability (and thus the inductance) of ferrite cores decreases as the current increases. This effect also helps to avoid resonance. However, resonance can still occur when a reactive load is connected to the filter.

## III. DESIGN OF AN OVERVOLTAGE-PROTECTED LOW-PASS FILTER FOR THE MAINS

The discussion of the design of a low-pass filter that contains integral overvoltage protection is divided into three parts. First, the overvoltage protection and basic filter design will be discussed. Second, damping of resonances and safety considerations will be discussed. Third, an alternate design will be discussed for applications that require low line-to-ground leakage currents.

The metal-oxide varistor is widely recognized as a cost-effective voltage limiting device for use on the mains [9]. One of the features of these varistors is a parasitic capacitance, which is often between 0.5 nF and 5 nF, shunted across its terminals. This capacitance can be utilized to make the first stage of a low-pass filter, while also obtaining voltage limiting [10].

The circuit shown in Fig. 2 has two stages. The first stage uses nominally identical metal-oxide varistors, V1 and V2, to provide voltage limiting for common-mode transients. Both the hot and neutral conductors are clamped at some relatively small potential (e.g., 300 V to 500 V) from ground. Inductor L1 and varistor V1 form a nonlinear voltage divider for transient overvoltages with short

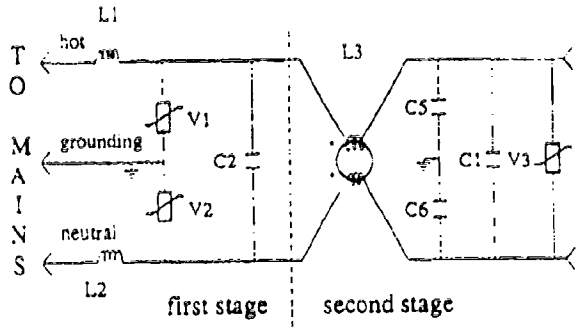


Fig. 2. Simple overvoltage-protected low-pass filter.

durations. L2 and V2 act in the same way for transients on the neutral conductor. For high-frequency noise, the inductances L1 and L2 form a low-pass filter with the parasitic capacitance of varistors V1 and V2 and with capacitor C2.

The second stage of the circuit shown in Fig. 2 contains a common-mode choke, L3, and bypass capacitors, C1, C5, and C6. The second stage of the low-pass filter shown in Fig. 2 attenuates the remnant of any transient overvoltage that passes downstream from varistors V1 and V2 and also provides additional attenuation of high-frequency noise. Components L3, C5, and C6 form a low-pass filter for common-mode signals. Owing to imperfections in the symmetry of the two coils in L3, this choke presents a relatively small inductance to differential-mode signals. This inductance and C1 form a low-pass filter for differential-mode signals. Additional protection from transient overvoltages is obtained by connecting varistor V3 as shown in Fig. 2.

There are many considerations involved in selecting component values for the circuit shown in Fig. 2.

The input inductors have a single layer construction to prevent insulation breakdown between layers and are rated to withstand at least a 5 kV impulse between terminals, as suggested by [11]. The single layer construction also increases the self-resonant frequency of the choke by decreasing the parasitic capacitance between the terminals. Chokes L1 and L2 are connected upstream from L3 because regular chokes can be more easily designed to withstand high-voltage transients than can common-mode choke L3.

The inductance values for L1 and L2 are limited by two considerations. These inductors are in series with the load current and have a voltage across them during the normal operation of the filter. If the filter is rated for 10 A rms, 60 Hz service and if a drop of 1 V rms across the filter can be tolerated, the maximum inductance is about 270 μH. This inductance limit applies to the sum of inductances L1 and L2, and the inductance of the choke L3 for differential-mode currents. Subject to this limit, larger values of inductance are more desirable.

Size is the other consideration for inductance value. The input inductors, L1 and L2, should have single layer construction. These inductors should be able to withstand at least 5 kV across the terminals. The high-voltage construction of these inductors will make them relatively large: a length between 7 cm and 12 cm is typical of single layer chokes with ferrite cores, an inductance between 10 μH and 80 μH, and a 20 kV rating. Since devices with larger inductance values have a larger size and there are size constraints on the completed filter module, the size of the module may determine the maximum practical inductance value for L1 and L2.

All lumped element capacitors have a small parasitic inductance, which may be as small as 5 nH, that makes the capacitor useless at high frequencies. It is well known that the parallel connection of two different capacitors (e.g., 0.5 μF and 0.01 μF) will provide a smaller magnitude of impedance over a wider frequency range than either capacitor alone [7]. The parasitic capacitance of the varistor V3 is effective in this way with capacitor C1.

A. Varistor Specifications

It is important that V1 and V2 be nominally identical devices. If the varistor connected between the neutral and grounding conductors, V2, were to have a smaller conduction voltage than V1, then common-mode transient overvoltages and noise would be converted to differential-mode by the mismatched varistors. Owing to the use of a common-mode choke, L3, with its large value of inductance in the second stage of the filter, the common-mode attenuation can be greater than the differential-mode attenuation. Therefore, it is desirable to have nominally identical devices for V1 and V2. There is also the prospect of having an application where the hot and neutral conductors are reversed in the wall outlet, so that V2 is exposed to the full mains voltage.

It is recommended that varistors for use on mains with a nominal voltage of 120 V rms meet the following specifications:

(1) When $V_N$ is the varistor voltage at 1 mA dc current and at a temperature of 25° C, the value of $V_N$ should satisfy
$$210 < V_N < 300 \text{ V}$$
(2) There should be less than 500 V across the varistor during an 8/20 μs test current with a 100 A peak value.
(3) The varistor should survive an 8/20 μs waveshape with a peak current of at least 5 kA without rupturing the case or loss of protective function.
(4) The varistor should be able to tolerate at least a million pulses of 50 A peak current (8/20 μs waveshape) without changing $V_N$ by more than ±10%.

For long-term reliability, there should be small power dissipated in the varistor when the rms voltage is somewhat greater than normal (F. Martzloff, personal communication). For this reason, the first specification has a larger minimum value of $V_N$ than might otherwise appear necessary.

With ZnO varistor technology available in 1987, such a varistor will have a minimum diameter of 20 mm. In the circuit shown in Fig. 2, varistors V1 and V2 are expected to be exposed to larger surge currents and therefore suffer more rapid degradation. Therefore, one could specify that varistors V1 and V2 have somewhat greater conduction voltage than varistor V3. Alternately, the first two varistors may be specified to have a larger diameter than varistor V3. For example, V1 and V2 might have a diameter of 32 mm, while V3 might have a diameter of 20 mm.

The clamping voltage for differential-mode transients at the input of L3 is twice the common-mode value, since V1 and V2 are in series for differential-mode voltages. This peak voltage value is unlikely to damage the dielectric of the capacitors, C1, C2, C5, or C6, or the insulation of the choke, L3. While it is no longer critical that the capacitors in this filter be able to withstand high-voltage transients, it is recommended that only capacitors with self-healing dielectrics that are rated for operation at 600 V dc (or more) be used. This provides a greater reliability for the filter.

B. Suppression of Resonances

The filter shown in Fig. 2 will have voltage gain at various frequencies owing to resonances of various LC pairs. There is a resonance for common-mode signals owing to L3, C5, C6, and the parasitic capacitances of V1 and V2. Another resonance for common-mode signals is owing to L1, L2, and the parasitic capacitances of V1 and V2. There is a resonance for differential-mode signals owing to L1, L2, C1, C2, and the non-ideal inductance of L3 to differential-mode signals.

As mentioned earlier, the possibility exists that the filter-load system will have resonances when a reactive load is connected to a low-pass filter. There are two possibilities for reactive loads: inductive and capacitive. Pure inductive loads are unusual. Most inductive loads across the mains (e.g., motors, relay coils) have substantial serie resistance that will act to damp any resonances. However, high-quality capacitive loads do exist: many pieces of electronic equipment have capacitors connected to the mains for suppression of electromagnetic noise. Many products intended for office and industrial applications have conventional low-pass filters connected to the mains, which have a capacitive input (see Fig. 1). Many electronic products for consumer applications (e.g., television receivers, video tape recorders, stereo receivers, etc.) have simple capacitors across the mains.

Voltage gain can be avoided by adding resistive dampening, as shown in Fig. 3. The circuit shown in Fig. 3 includes all of the components shown in Fig. 2, plus seven resistors and two capacitors.

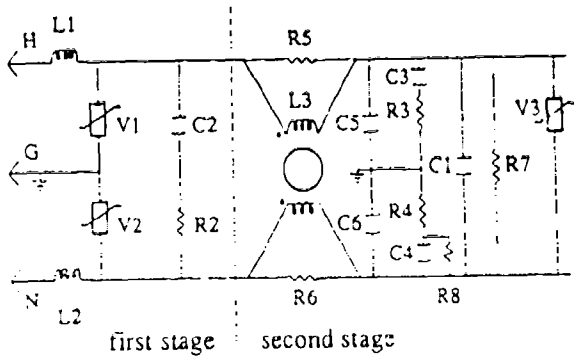


Fig. 3. Overvoltage-protected filter for commercial use.

Given the types of reactive loads in the world, one cannot suppress resonances in a low-pass filter by merely connecting resistors in series with shunt capacitors inside the filter. While this would damp internal resonances, it does nothing to solve the resonance owing to the external capacitive load. Instead, resistors, such as R5 and R6 in Fig. 3, are shunted across the inductor nearest the output port. A crude initial approximation for the value of these resistances can be obtained by calculating the reactance of one coil in L3 at the resonance frequency.

It is undesirable to connect resistors in parallel with L1 and L2 because these inductors may be exposed to high-voltage transients that might damage inexpensive resistors.

The series RC networks shown in Fig. 3 provides damping of resonances. Such networks are common in switching applications with relays, SCRs, or triacs, where they are known as "snubber networks." Resistor R2 damps the resonance to differential-mode signals formed by L1, L2, C2, C1, and the differential-mode inductance of L3. The snubber networks R3,C3 and R4,C4 provide damping of resonances of common-mode signals owing to L3, C5, and C6. Further damping for both differential- and common-modes may be provided by the resistive component of the impedance of L1, L2, and L3 owing to the losses in the cores of these chokes.

There is no reason to include a damping resistor in series with C1, since a capacitive load would remove the effect of this resistance. The use of damping resistor R2 can adequately suppress differential-mode resonances.

Resistor R7 is included to discharge the capacitors if the filter is disconnected from the mains with no load present. The value of R7 may be chosen to decrease the potential across capacitors C1 and C2 to some small value (e.g., less than 30 V) one second after the mains are disconnected at a positive peak of the sinusoidal mains waveform. There is no need to discharge capacitors C5 and C6 because their capacitance is so small. If C3 and C4 have large capacitances, another discharge resistor, R8, should be included. The resistances of R7 and R8 are too large to have an effect on damping of resonances; these resistors are included only for safety considerations.

## IV. DESIGN OF AN OVERVOLTAGE-PROTECTED MAINS FILTER FOR PATIENT CARE EQUIPMENT

A filter can be designed for medical equipment in patient care applications using the principles discussed above. The only unusual criterion is that of very low leakage current (see Table 1). If a generous safety margin is to be provided, the line-to-ground capacitance must be limited to about 500 pF, which effectively prohibits the use of either metal-oxide varistors or large capacitances in line-to-ground connections. Some of these difficulties can be overcome with the circuit shown in Fig. 4.

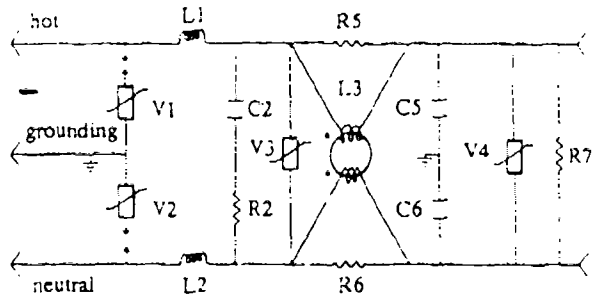


Fig. 4. Overvoltage-protected filter for patient care equipment.

The relatively large parasitic capacitance of the line-to-ground varistors, V1 and V2, is reduced to only a few picofarads by connecting a spark gap in series. However, the spark gap has a delay time between the application of an overvoltage and the onset of an arc inside the gas. By placing the spark gaps and varistors upstream from chokes L1 and L2, we obtain two advantages. First, the inductance in L1 and L2 helps create a large voltage during transient overvoltages with a short rise time, which will

reduce the delay time in the spark gaps. Second, the low-pass filters formed by the various inductors and capacitors attenuate the remnant that passes downstream from the spark gaps, V1, and V2. Prior to the onset of the arc inside the spark gaps, this remnant will be the entire transient overvoltage across the input port. This idea is not new: [11] advocated it thirty years ago. However, the merits of this circuit appear to have been ignored.

The selection of varistor models for this circuit is guided by the same principles that were discussed above for a commercial environment. Use of a varistor that is suitable for direct connection between the mains and ground will cause the spark gap to extinguish when the overvoltage ceases; there will be no "follow current."

Attenuation of differential-mode overvoltages is provided by chokes L1 and L2, together with varistors V3 and V4. A differential-mode low-pass filter is formed by L1, L2, and C2. Resonance is suppressed by including resistor R2 in the middle of the filter. Additional attenuation of high-frequency differential-mode signals is provided by the parasitic capacitances of V3 and V4.

A common-mode low-pass filter is formed by common-mode choke, L3, and capacitors C5 and C6. For safety reasons, the capacitance of C5 and C6 is limited to about 500 pF each.

The purposes of R5, R6, and R7 in Fig. 4 are identical to the components of the same designations in Fig. 3, which were explained above.

## V. TESTS

Prototype versions of the overvoltage-protected filters for use in either a commercial or medical environment were subjected to a number of different tests in a laboratory. The steady-state frequency response is presented first. Then the response to transient overvoltages is discussed.

### A. Steady-State Frequency Response

Attenuation as a function of frequency was measured with the circuit shown in Fig. 5. The signal source was a Wavetek model 191 function generator that was connected to an Amplifier Research model 50A15 power amplifier. This combination could provide a sinusoidal waveform over the frequency range from 10 kHz to 20 MHz. Nearly all of the data were collected with a 20 V peak-to-peak sinusoidal input signal. The voltmeters were the two channels of a Tektronix model 2445 oscilloscope, which have an input impedance of 1 MΩ shunted by about 15 pF. A 50 Ω coaxial load was connected at the front panel of the oscilloscope for the measurement of voltage across the filter's output port. Coaxial cable was used for all connections. Frequency measurements were made with the cursors on the oscilloscope screen.

It was not possible to measure the differential-mode response of the filter, since a high-quality, center-tapped transformer with a wide bandwidth was not available. A crude substitute was to connect the neutral to ground at both the input and output ports, which gives what may be called the "normal-mode" response. Since one terminal of the oscilloscope input is at ground potential, no other choice was possible.

Fig. 6 shows the frequency response for the low-pass filter for commercial environments, which uses the schematic shown in Fig. 3. The solid line shows the response to common-mode signals; the dashed line shows the response to normal-mode signals. The resonance near 0.8 MHz is caused by the inductances of L1, L2, and the parasitic capacitances of V1 and

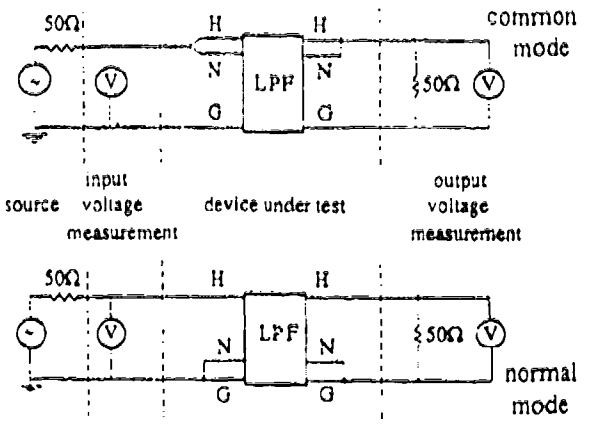


Fig. 5. Schematic for frequency response measurements.

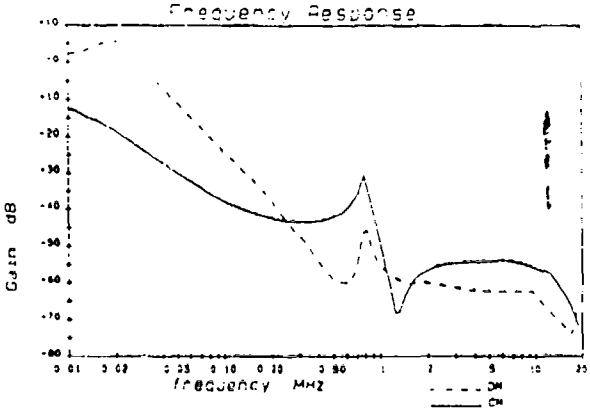


Fig. 6. Frequency response of the filter for commercial environments.

V2. The resonance for normal-mode signals near 20 kHz is caused by L1, L2, and C2.

Fig. 7 shows the frequency response of the low-pass filter for medical environments, which uses the schematic shown in Fig. 4. The attenuation of common-mode signals at frequencies below about 0.1 MHz is mostly due to voltage division using the inductance (L1, L2, and L3) and the 50 Ω resistive load at the oscilloscope input. This is not surprising, since there is a stringent limit on the maximum value of line-to-ground capacitance in this environment. The amount of attenuation of normal-mode signals of this filter is similar to that of the filter for commercial environments.

### B. Response to Transient Overvoltages

The response to transient overvoltages of various low-pass filters for use on the mains was tested, using the schematic diagrams shown in Fig. 8. The overvoltages were supplied by a Keytek model 424 surge generator. The response was monitored by a Tektronix model 7612D digitizer with two 7A13 amplifiers with differential inputs. The voltage

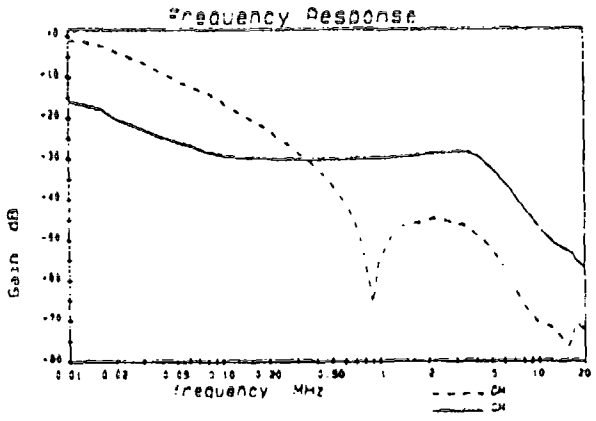


Fig. 7. Frequency response of the filter for medical environments.

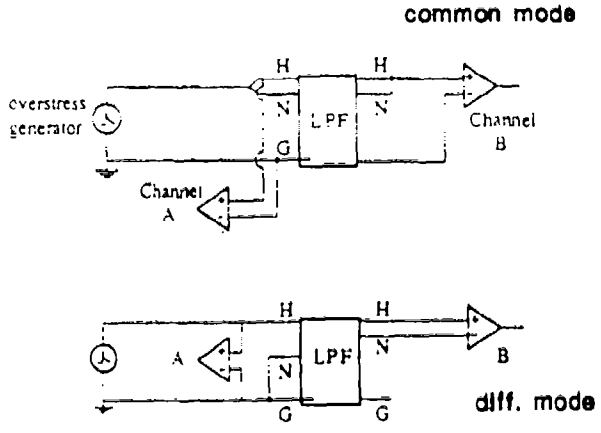


Fig. 8. Schematic for exposure to transient overvoltages.

across the input port of the filter was measured with a pair of Tektronix P6015 probes; model P6009 probes were used to measure the voltage across the output port. Use of a pair of probes and a true differential amplifier eliminates errors owing to changes in ground potential during the application of the overvoltage. The probes were properly compensated in the usual way. Then the common-mode rejection ratio was maximized by adjusting the compensation of the reference probe (the one connected to the inverting input of the amplifier) to give the minimum differential signal when both probes were connected simultaneously to the same output of a rectangular pulse generator.

The two cables for the P6015 probes were twisted together and secured with plastic spiral wrap. This reduces the amount of error voltage induced on the cables by rapidly changing magnetic fields during surge testing. The two P6009 probes had their cables twisted together and secured in the same way.

All surge testing was done with a 0.5 μs-100 kHz ring wave, which is defined in ANSI C62.41-1980.

The filter under test was connected to the 120 V rms, 60 Hz mains through a back-filter. The internal back-filter in the Keytek model PN281 programmer

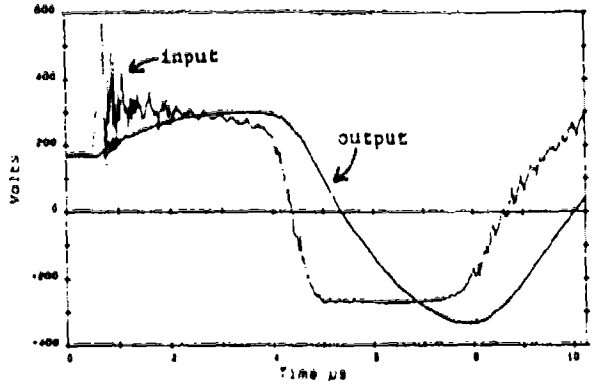


Fig. 9. 1 kV open-circuit common-mode ringwave applied to medical filter.

network was used. Additional protective devices (metal-oxide varistors and low-pass filters) were placed upstream from this back-filter for increased assurance that equipment elsewhere in the building would not be damaged or upset by this testing. Because the filter is designed to be connected to the mains during normal use, it is important to test it when energized by the mains voltage.

In order to observe a worst-case condition, no load was used during these tests. While this is not the typical way to use a filter, it does present a worst-case. A low-pass filter is built with a large series impedance and a small shunt impedance. Use of any capacitive load at the output port will decrease the shunt impedance and increase the attenuation. Use of a purely resistive load is likely to damp any resonances.

The major concern during the design of the low-pass filter for use in medical environments was whether the filter would provide adequate attenuation of the remnant that travels downstream from the spark gaps and varistors V1 and V2 in Fig. 4. The worst-case for passage of a remnant occurs when the voltage across the input port has a slow rate of rise, so that the spark gaps are relatively slow to conduct and the remnant has a relatively long duration. The worst-case can be worsened further by applying a common-mode transient overvoltage, since the attenuation of the filter is markedly less for common-mode signals owing to limits on the maximum line-to-ground capacitance.

Fig. 9 shows the common-mode voltages across the input and output ports of the filter for medical environments. The surge generator was set to provide a peak open-circuit voltage of about 1 kV. The voltage at the left edge of Fig. 9 is about 170 V, the peak of the mains voltage. The surge is applied and the voltage across the input port increases at an average rate of 1.9 kV/μs. At least one of the gaps conducted when the voltage across it and its series varistor was 575 V. The voltage across the input port decreases abruptly to about 220 V and behaves in a very noisy manner. The times of the peaks in this noise were reproducible from one test to another, so they probably arise from reflections from the various protective devices upstream from the back-filter and from nodes inside the filter under test. The peak current from the surge generator, measured by an ammeter inside the surge generator, was 14 A. This was a very mild stress.

The voltage across the output port of the filter is much smoother and of a generally smaller amplitude than the voltage across the input port. At the left

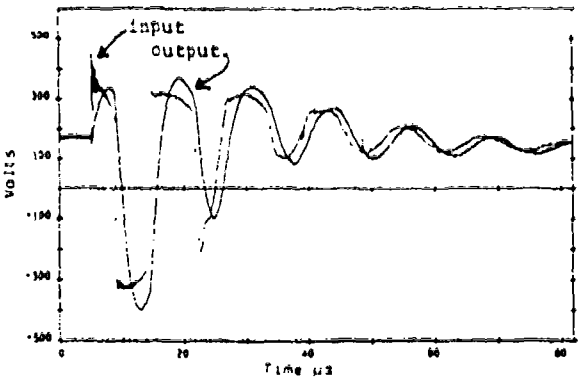


Fig. 10. 6 kV open-circuit common-mode ring wave applied to medical filter.

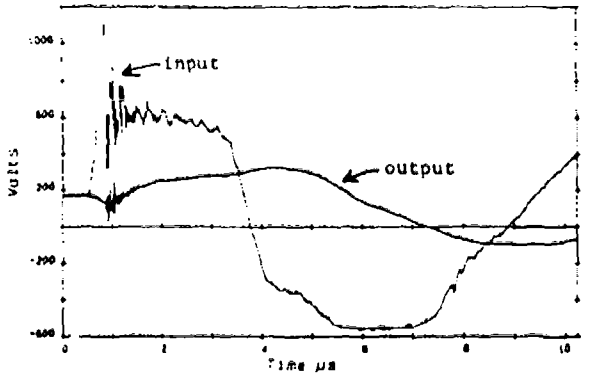


Fig. 11. 1.5 kV open-circuit differential-mode ring wave applied to medical filter.

edge of Fig. 9, the voltages across the input and output ports have the same value, as would be expected, since there is negligible loss in the filter at the frequency of the ac mains. When the gap(s) sparked over, the voltage across the output port had an oscillation with a peak-to-peak value of about 50 V. This oscillation may be due to radiated electromagnetic noise from the large value of dI/dt in the spark gap(s). Neglecting these oscillations, the initial rate of change of the voltage across the output port was about 0.08 kV/µs, about 4% of that across the input port. The voltage across the output port is greater than that across the input port at times near 4 and 8 µs. There is no common-mode voltage clamping at the output of this filter, so such an outcome is possible.

Fig. 10 shows a larger common-mode overstress test of the same filter. The surge generator was adjusted to give a peak open-circuit voltage of about 6 kV. The digitizing rate was slowed to capture the entire ring wave. The greater initial value of dV/dt across the input port caused the spark gap(s) to conduct at a lower voltage than in the test shown in Fig. 9. This is to be expected: it is well known that spark gaps conduct more quickly when | dV/dt | is greater. The peak current drawn from the surge generator was 180 A. The common-mode voltage across the output port is clamped at 400 V in this test.

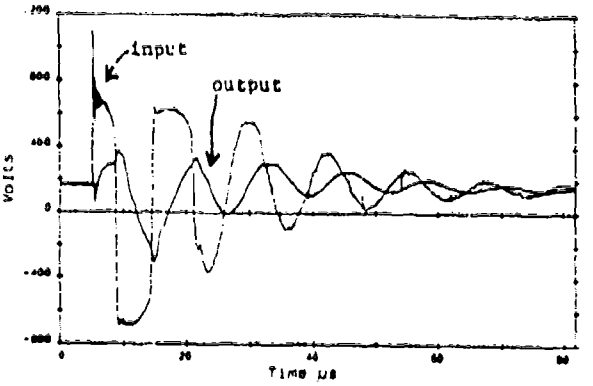


Fig. 12. 6 kV open-circuit differential-mode ring wave applied to medical filter.

Fig. 11 shows a mild differential-mode ring wave test. The surge generator was adjusted to give a peak open-circuit voltage of about 1.5 kV. The peak voltage across the input port, about 1.1 kV, is greater than that in Fig. 9 because the two spark gaps and varistors V1 and V2 were in series with the surge generator, unlike the common-mode test in Fig. 9. The value of dV/dt across the input port prior to sparkover was about 2.9 kV/µs. The peak current drawn from the surge generator was 16 A; this was a mild stress. The voltage across the output port is much smoother than the voltage across the input port. Since the attenuation of differential-mode signals is greater than the attenuation of common-mode signals for this filter, it is not surprising that the voltage across the output port is smoother in Fig. 11 than in Fig. 9.

Fig. 12 shows a greater differential-mode overstress test of the same filter. The surge generator was adjusted to give a peak open-circuit voltage of about 6 kV. The digitizing rate was slowed to capture the entire ring wave. The peak current drawn from the surge generator was 164 A. The differential-mode voltage across the output port is clamped at 360 V in this test.

Further tests were planned with (1) this overvoltage-protected filter for a medical environment, (2) an "off-the-shelf" low-pass filter module that has no overvoltage protection, and (3) the overvoltage-protected filter for commercial environments that was described in Fig. 3. The nonprotected filter was tested next with the same experimental arrangement that was described above. A differential-mode ring wave with an open circuit voltage of 6 kV produced insulation breakdown in the line-to-neutral capacitor inside the filter. Enough energy and voltage reached the output port of this filter to damage the amplifier in the digitizer. The amplifier could not be repaired in time to prepare additional figures for this paper. This unfortunate result does show that including overvoltage protection in filters can reduce the incidence of damage to sensitive electronic circuits!

## VI. CONCLUSIONS

Many kinds of devices have been recommended by engineers to protect vulnerable equipment from disturbances on the mains, including noise and high-voltage transients. These devices include isolation transformers, line conditioners, ac voltage

regulators, and motor generator sets [12]. These devices are expensive: a unit that is rated for service at 120 V rms, 500 VA costs at least $400. In many applications regulation of the ac mains voltage is no longer critical. For example, many switching power supplies that are intended for use on nominal 120 V rms mains will operate reliably with any input voltage between 80 and 130 V rms. Common desktop computer systems use switching power supplies and do not require a regulated ac mains voltage. When ac voltage regulation is not needed, a low-pass filter that includes protection from transient overvoltages may be an acceptable substitute for more expensive devices such as line conditioners. When isolation at dc and the frequency of the mains is not required, the common-mode choke in a low-pass filter may be an acceptable substitute for noise reduction by isolation transformers. Providing critical loads, such as computer systems, with protection from transient overvoltages and noise would be expected to reduce the upset and damage rate for the systems.

Acknowledgments - The analysis and design of the filters described in this paper was supported by the U.S. Army Research Office under contract DAAL03-87-K-0078. Financial support for development and testing of prototype filters was provided by the Allegheny Power System and Joslyn Electronic Systems. The author thanks all of these sponsors.

## REFERENCES

[1] F. D. Martzloff and G. J. Hahn, "Surge Voltages in Residential and Industrial Power Circuits," IEEE Transactions on Power Apparatus and Systems, July 1970, vol. 89, pp. 1049-1056.

[2] R. B. Standler, "Transients on Mains in a Residential Area," submitted to IEEE Trans. EMC.

[3] J. H. Bull, "Voltage Spikes in Low Voltage Distribution Systems and Their Effects on the Use of Electronic Control Equipment," Electrical Research Association Report Nr. 5254, Leatherhead, Surrey, May 1968.

[4] H. M. Schlicke and H. Weidman, "Compatible EMI Filters," IEEE Spectrum, vol. 4, Oct 1967, pp. 59-68.

[5] L. W. Ricketts, J. E. Bridges, and J. Miletta, EMP Radiation and Protective Techniques, John Wiley, 1976, 363 pp.

[6] V. Kübel, "Characteristics and Application of Radio Interference Suppression Filters with Current Compensated Chokes," Components Report, vol. 10, no. 4, Oct 1975, pp. 108-111.

[7] R. B. Standler, Transient Protection of Electronic Circuits, U.S. Air Force Weapons Laboratory Technical Report, AFWL-TR-85-34, 1984, 212 pp.

[8] Underwriters Laboratory Standard 1283, "Electromagnetic Interference Filters," revised second edition, Feb 1986.

[9] J. D. Harnden, F. D. Martzloff, W. G. Morris, F. G. Golden, "Metal-Oxide Varistor: a new way to suppress transients," Electronics , 9 Oct 1972, pp.91-95.

[10] M. Campi, "EMP Circuit Board Filter Using MOV Devices," U. S. Patent 4,021,740; 3 May 1977.

[11] J. B. Hays and D. W. Bodle, "Electrical Protection of Tactical Communication Systems," Bell Laboratories Technical Report, Aug 1958. (Available from National Technical Information Service, catalog Nr. AD-693300)

[12] R. B. Standler and A. C. Canike, Mitigation of Mains Disturbances, Air Force Weapons Laboratory Technical Report AFWL-TR-86-80, July 1986, 192 pp.

# WIDEBAND OVERVOLTAGE PROTECTION CIRCUIT

Daniel R. Shakarjian, MEMBER

Ronald B. Standler, SENIOR MEMBER

Department of Electrical Engineering

The Pennsylvania State University

University Park, PA 16802

## ABSTRACT

We report the development, design, and performance of an overvoltage protective circuit that has a signal bandwidth from dc to 200 MHz, is matched to the impedance of a 50 Ω transmission line in order to avoid reflections during normal operation, and clamps the voltage across the protected port to less than 16 V during a surge with a 8/20 μs waveshape and a peak current of 3 kA. This overvoltage protective circuit has applications in protecting high-speed computer local area networks (LAN), the antenna input port of radio receivers, and inputs of oscilloscope vertical amplifiers.

## INTRODUCTION

An important problem in the design of overvoltage protection has been to protect computer local area networks (LANs) from damage by lightning. Common LANs transmit rectangular pulses at a rate of the order of $10^7$ pulses per second. A bandwidth of at least 50 MHz, and preferably 100 MHz, is desirable for circuits connected to LANs. Another important problem is protection of military radio receivers from damage by either the electromagnetic pulse produced by detonation of nuclear weapons or by high-power microwave weapons. A third application would be protection of inputs of wideband vertical amplifiers in oscilloscopes.

A review of the previously reported ways to protect electronic equipment from damage by surges on data and signal lines, with concentration on the properties of these protective circuits at high frequencies, shows that there are few acceptable devices for a broadband overvoltage protection circuit (Standler, 1989). Spark gaps and silicon avalanche diodes are well-known as components that are useful to protect electronic systems from damage by transient overvoltages. However, each of these components have disadvantages that may make it unsuitable when used alone to protect modern integrated circuits. Spark gaps require a time between $10^{-9}$ and $10^{-3}$ s to conduct, depending on the rate-of-change of the voltage across them. Prior to conduction the full overvoltage, which can have a peak value in excess of 1 kV, can propagate downstream past the spark gap. This large remnant can damage vulnerable semiconductors. Avalanche diodes alone can be damaged by relatively small surge currents (e.g., 500 A for an 8/20 μs waveform), but have fast response. In order to survive large surge currents, the cross-

sectional area of the diode must be large in order to reduce the current density. The large area makes the parasitic capacitance large. The large parasitic capacitance of avalanche diodes makes them unsuitable when used alone for a broadband protection circuit.

## HYBRID CIRCUIT

Bodle and Hayes (1957) first described the combination of a spark gap and avalanche diode in the so-called "hybrid" circuit shown in Fig. 1. The highly nonlinear V-I characteristic of the avalanche diode can provide tight clamping of the voltage across the protected port. When a large current surge current passes through the series impedance, $R + j\omega L$, and the avalanche diode, a large voltage appears across the spark gap. This large voltage causes the gas in the spark gap to ionize and the spark gap shunts current away from the avalanche diode. In this circuit the avalanche diode protects the devices downstream, while the series impedance and the spark gap protect the avalanche diode (Standler, 1989). Some implementations of this circuit omit either the resistance or the inductance (but not both) in order to reduce cost or space.

Typical values of resistance, R, range between about 3 and 22 Ω. When inductance is used alone, typical values of L are of the order of 30 μH.

The series impedance forms a low-pass filter with the parasitic capacitance of the avalanche diode. A typical value of the parasitic capacitance of a 6.8 V avalanche diode that is designed for conduction of surge currents is 10 nF. The combination of a 10 Ω series resistance and a

10 nF shunt capacitance makes a low-pass filter with a corner frequency of about 1.6 MHz. In addition to the attenuation of high-frequencies, the circuit of Fig. 1 is a poor match to the characteristic impedance of a transmission line so that reflections will be produced. This circuit is not suitable for protecting circuits that must routinely carry high-frequency signals.

## MATCHED CIRCUIT

Fig. 2 shows a circuit described by Schlicke (1974) that uses the parasitic capacitance of a metal-oxide varistor, C, and a series inductor, L, to build a single lumped-element approximation of a transmission line that has a characteristic impedance $Z_o$. The protective circuit is matched to the impedance of the transmission line when Eqn. 1 is satisfied.

$$Z_o = \sqrt{L/C} \qquad (1)$$

This matching would seem to eliminate reflections from an impedance discontinuity at the transmission line--protective circuit interface. However, the circuit in Fig. 2 does little to extend the bandwidth of the system. If C is 10 nF, then L must be 25 μH to provide a match to a 50 Ω transmission line. This combination of L and C makes a low-pass filter with a corner frequency of 0.6 MHz and a slope in the stop-band of -12 dB/octave (instead of the -6 dB/octave slope of a single RC low-pass filter). The circuit of Fig. 2 may provide <u>more</u> attenuation at high frequencies than the circuit in Fig. 1. Both circuits are undesirable in applications that require wide bandwidth.

## DESIGN AND CONSTRUCTION OF OUR CIRCUIT

We report here the development, design, and performance of a modified hybrid protective circuit that has a signal bandwidth from dc to nearly 200 MHz and can easily survive surge currents with an 8/20 μs waveshape and a peak value as large as 3 kA. The schematic diagram of this protective circuit is shown in Fig. 3. After a search of semiconductor catalogues, computer-aided design, building, and testing several prototypes, the parts in Table 1 were chosen for a wideband protective circuit matched to a 50 Ω transmission line.

The spark gap, series impedance, and diode $D_1$ follows the traditional design shown in Fig. 1. The final inductor-capacitor section in Fig. 3 uses an inductor and parasitic capacitance of nonlinear shunt elements in a way similar to the circuit shown in Fig. 2. The rectifier diode $D_2$ in Fig. 3 is included to reduce the shunt parasitic capacitance provided by $D_1$ in order to extend the bandwidth (Popp, 1968; Clark and Winters, 1973). In addition to having a small capacitance, rectifier diodes $D_2$ and $D_3$ must have a small forward voltage drop at high surge currents and fast turn-on time. Since $D_2$ prevents $D_1$ from conducting during negative polarity, the rectifier diode $D_3$ is included to provide clamping of the output port during negative polarity surges.

The series inductance is determined by Eq. 1 in order to match the impedance of the transmission line. To match the network to a characteristic impedance of $Z_0 = 50\ \Omega$, the value of $L_3$ would have to be 50 nH for a total diode capacitance of 20 pF. In Fig. 3, the total value of

impedance $j\omega(L_1 + L_2 + L_3)$ between the spark gap and $D_1$ is too small to provide proper coordination during surges with durations of at least tens of microseconds (e.g., 8/20 μs wave shape). Therefore, it was necessary to insert a small resistance, R, to limit the current in the avalanche diodes and cause the spark gap to conduct during surges.

In order to improve the match between the protection circuit and the transmission line a cascade of two passive inductor-capacitor sections, $L_1/C_1$ and $L_2/C_2$, were inserted as shown in Fig. 3 and as suggested by Garver (1976).

Since the protection module is to be used to pass VHF frequencies, the components must have good high frequency characteristics. For example, ferrite-core inductors would be too lossy, so air-core inductors were used. The air-core inductors were formed by winding copper wire with a diameter of 0.5 mm and plastic insulation into a single-layer coil of a few closely-spaced turns with an inside diameter of 2.5 mm. The single-layer construction reduces the parasitic shunt capacitance and raises the self-resonant frequency of the inductor.

Our prototype circuit used devices in conventional packages, rather than surface mount devices. Initially we were concerned that the diodes should have a large surge current rating and that $C_1$ and $C_2$ should have a large voltage rating. We were not able to obtain such components in surface mount packages.

Magnetic fields from the surge current upstream from and inside the

spark gap can induce undesirable voltage across the protected port by coupling into loop area downstream from the gap (Ter Haseborg and Trinks, 1984; Standler, 1989). By placing the spark gap in a coaxial mounting in a separate package upstream from the remainder of the circuit shown in Fig. 3, we avoided the adverse effects of the radiated magnetic field from spark gap currents.

As with any high-frequency circuit, component placement is critical. The inductors $L_1$, $L_2$, $L_3$ had a common axis to mimic a continuous transmission line.

## rf model for the diodes

We determined the component values for the circuit in Fig. 3 to maximize the bandwidth and minimize the VSWR of the circuit in the passband. To do the design, it is necessary to have a model of the diode network, including parasitic elements, that is valid at radio frequencies.

Diodes $D_1$, $D_2$, and $D_3$ (connected as shown in Fig. 3) have a complex impedance that is mostly capacitive at frequencies below 40 MHz, with a small resistive part. The parasitic inductance and capacitance of the diodes provides a self-resonant frequency of the order of 500 MHz. At frequencies higher than the self-resonant frequency, the diodes' lead and package inductance dominates and the impedance is all inductive.

To develop an appropriate diode model at VHF and UHF frequencies, a diode network consisting of $D_1$, $D_2$, and $D_3$ were connected to a Hewlett

Packard model 8510A Network analyzer. The lead lengths were kept as short as possible in order to minimize the parasitic inductance and thus increase the self-resonant frequency. Short leads also minimize the inductive voltage rise that occurs for large values of di/dt of transient overstresses. The lead lengths were only long enough to allow the diodes to be soldered to the circuit card. The diodes' scattering parameters were measured from 45 MHz to 1000 MHz. A sinusoidal signal with an amplitude of 0.4 V across $D_3$ and a dc bias of +2 V were chosen to insure that the diode network was not forward biased for either polarity of input signal. Measurement of the scattering parameters revealed the frequencies at which the diode network had series and parallel self-resonances. A series resonance occurs at about 460 MHz and a parallel resonance at 780 MHz. The value for the parasitic inductance of the network of all three diodes is approximately 6 nH.

A better approach in determining the parasitic diode elements was accomplished with the aid of microwave CAD software. Touchstone, a microwave CAD program from the EESOF company, was used to generate the "best fit" parasitic elements by comparing the model's s-parameters to those obtained from measurement. The element values are then iteratively found from the s-parameters.

## small-signal rf performance

Depending on the particular application, the bandwidth and input VSWR of the protection network can vary. For applications involving small signals with a voltage between -0.5 and +0.5 V, the measured passband of the protection network extends from dc to 198 MHz in a 50 Ω system. The insertion loss is 0.5 dB at 100 MHz and the VSWR at port 1 is less than 1.5 from dc to 160 MHz.

The 3 Ω resistor, R, contributes 0.25 dB of insertion loss throughout the passband. If this loss is objectionable, then a small capacitance could be placed in shunt with R.

For applications involving larger signals, the diodes exhibit slightly different characteristics. Under different dc bias, the diodes' capacitance varies and the fixed parameters in the design model are not valid. In order to characterize the performance of the circuit as a function of bias voltage, a series of measurements were made with a Hewlett-Packard Model 8510A network analyzer. We used a sinusoidal signal with an amplitude of 0.4 V across $D_3$ and a dc bias of 2, 3, and 4 V. The forward transmission, VSWR at each port, and phase response, all as a function of frequency and dc bias voltage, are shown in Figs. 4--7.

As shown in Fig. 4, the bandwidth decreases as the bias voltage increases. With a +4 V bias, the bandwidth is 131 MHz, about 66% of the bandwidth at zero bias.

As shown in Fig. 5, the frequency at which the VSWR at port 1 is 1.5 is about 158 MHz for bias voltage of 0, 2, or 3 V. However, the VSWR at port 1 is less than 1.5 for frequencies less than 66 MHz when the bias voltage is 4 V. The VSWR at port 2, which is shown in Fig. 6, is slightly larger than at port 1.

As shown in Fig. 7, the phase response is approximately independent of bias voltage between 0 and 4 V. The phase response shows the self-resonant frequency of the protection circuit.

The protection circuit may also be useful as a low-pass filter, for example to prevent aliasing by an analog-to-digital converter and to prevent upset of systems connected to port 2 by noise or the remnant of a transient overvoltage. Measurement of $S_{21}$ shows that the transmission is less than -32 dB for frequencies between 400 MHz and 1 GHz, with a dc bias of 0, 2, 3, or 4 V.

It would be highly beneficial if the protection module could perform equally well in the reverse transmission mode: when a signal is transmitted from the protected port (port 2) to port 1. A bidirectional network is well suited for digital data line transmission and reception such as those found in local computer network links or other bidirectional data buses. When this circuit is used in the reverse transmission mode, both the bandwidth and the phase response remain unchanged. However, the reflection coefficient at port 2 is not the same as that of port 1. The transmitting source sees a slightly different impedance and so the VSWR is altered slightly. To make the optimal bidirectional circuit, the circuit should be

symmetrical: the protection diodes should be placed in the middle section of the filter, as shown in Fig. 8, rather than at the end.

Use of surface mount diodes would reduce the parasitic inductance in those devices and improve the rf performance of the circuit. We expect that coating the interior of the shielded box that contained the circuit with a compound that absorbs electromagnetic radiation would improve the rf performance of the circuit, because removing the metal box increased the attenuation above 400 MHz by about 10 dB.

This circuit was originally designed for protection of computer local area networks that have a signal level between 0 and 5 V. The input of a radio receiver would have a smaller range of signal levels, so diode $D_1$ would not be necessary for that application. There are many variations on the circuit in Fig. 3 that would be appropriate for different applications.

## Surge Performance: large currents

To determine the clamping voltage across the protected port, a number of different tests were performed with surge currents applied to port 1. The test schematic is shown in Fig. 9.

Surges with a short-circuit current waveshape of 8/20 μs were generated by either a Keytek model 424/PN 242 generator or a Haefely model PC-6-288 generator. The Keytek was used for peak currents between 50 and 500 A; the Haefely for currents between 0.5 and 3 kA. The current in port 1 was measured with an Ion Physics model CM-10-L current transformer. The voltage

across the protected port was measured with Tektronix P6009 probes The data were recorded with a Tektronix model 7612D programmable digitizer with two 7A13 amplifiers. The digitizer samples both channels simultaneously at a maximum rate of one sample per 5 ns. The digitizer was typically programmed to record 128 samples prior to the trigger event and 1920 samples after the trigger event.

Fig. 10 is a plot of the output port voltage and input port current vs. time. The applied input surge is the 8/20 μs current waveform with a peak at +535 A. The first 2.4 μs of the surge illustrates clamping of the diode array alone. When the input current reaches 86 A there is 258 V across the 3 Ω series current limiting resistor, R, and there is enough potential difference across the the spark gap to cause the spark gap to conduct. When the spark gap conducts, the surge current increases suddenly because the surge generator "sees" a lower impedance. The output voltage across the protected port is clamped to +11.3 V prior to the conduction of the spark gap. After the gap conducts and shunts current away from the diodes, the voltage across the protected port falls to about 8 V.

The circuit was also tested with an 3/20 μs waveform with a peak surge current of +3 kA. The maximum output voltage across the protected port was 15.9 V. The spark gap conducted 0.32 μs after the surge began. When the spark gap conducted the output voltage at the protected port decreased to about 8 V. The protection circuit survived repeated exposures to an 8/20 μs waveform with a peak current of 3 kA without detectable degradation of either the rf performance or the clamping voltage.

## Surge testing: blind spot

Because the diodes are the most vulnerable components in the circuit, it is critical to test the circuit with the maximum stress that the diode network can tolerate without the spark gap conducting, the so-called "blind spot". To determine the blind spot for a given surge waveform, a series of surge tests are conducted. If the spark gap conducts, the magnitude of the input current is reduced during the subsequent test. If the spark gap does not conduct, the magnitude of the surge current is increased during the subsequent test. For an 8/20 μs waveform, the largest peak current that would not cause the spark gap to conduct was between 72 and 75 A. The voltage across the output port is clamped to +10.4 V during the blind spot tests.

Surge currents of negative polarity were also applied to the protection network as shown in Fig. 10. For an 8/20 μs surge current with a peak of -72 A, diode $D_3$ clamped the voltage at -3 V. The blind spot current range was found to be the same as mentioned above. This is reasonable because during a surge of either polarity the magnitude of the voltage across port 2 is much smaller than the peak voltage across port 1. Thus, the spark gap does not "see" a significant difference in the magnitude of clamping voltage owing to conduction of $D_3$ during negative current surges or $D_1$ during positive current surges.

## Surge testing: nanosecond response

We measured the speed of response of our circuit with the test schematic shown in Fig. 11. We used a rectangular surge voltage waveform from a coil of 50 Ω coaxial cable with a one-way propagation time of 0.5 μs that was charged to between 0.5 and 1.0 kV and discharged into the circuit under test through a mercury-wetted relay. This generator had a rise time of 0.6 ns. A T&M coaxial resistor with a value of about 0.14 Ω was installed so that the current in port 1 could be measured. We observed the voltage across the protected port through a 10X coaxial attenuator. The waveforms were measured with a Tektronix model 7104 analog oscilloscope with a 7A29 vertical amplifier and a 7B15 time base. The manufacturer's specifications for these instruments give a system rise time of less than 0.35 ns. A photographic camera was used to record the CRT image.

A typical oscillogram of the voltage across port 2 as a function of time is shown in Fig. 12. The voltage across the protected port reaches a peak of 35 V, then decreases to a steady-state clamping voltage of about 8 V less than 10 ns after the stress begins. The actual peak voltage may be greater than that indicated in Fig. 12, due to limiting by the 1 GHz bandwidth of the oscilloscope.

The maximum voltage across the protected port was observed (with a sweep rate of 2 ns/div and a charging voltage of 1 kV) to be 62 V, which is much greater than that observed during stresses with 8/20 μs waveform. Such overshoot is a common feature of transient protection circuits, although such overshoot is often not observed simply because of inadequate bandwidth

in the oscilloscope, digitizer, or voltage divider and because of insufficient value of $|dV/dt|$ in the surge generator.

It is easy to understand why the clamping voltage is larger for a rectangular pulse than for an 8/20 μs waveform. The rectangular waveform used in this test has a value of dV/dt that is three orders of magnitude greater than that of the input voltage during the 8/20 μs waveform. The 8/20 μs waveform does not have a sufficiently large value of dV/dt to allow the response time of the diode network in our circuit to be measured.

There are two causes for the large clamping voltage for the first few nanoseconds of the overstress. A rectifier diode $D_2$ has a much longer response time than does the reverse-biased avalanche diode $D_1$ (Clark and Winters, 1973). The large packages of $D_1$ and $D_2$ have a total parasitic inductance of about 10 nH. This inductance prevents instantaneous conduction of the diodes. We attempted to minimize the response time of $D_2$ by specifying an "ultrafast" diode and connecting it with minimal lead length. Surface mount devices would reduce the parasitic inductance, but we do not know how to further decrease the turn-on time of $D_2$.

For this waveform, the largest short-circuit current was only 1 kV/50 Ω, or 20 A. With this small current it was not possible to observe a change in the voltage across the protected port when the spark gap conducted. By observing the voltage across port 1, we were able to determine that the spark gap conducted between 7 and 10 ns after the beginning of the rectangular pulse.

## CONCLUSION

The circuit shown in Fig. 3 has a lower input VSWR and has two orders of magnitude wider bandwidth than the traditional overvoltage protection circuits that were discussed in the introduction, while maintaining surge current handling capabilities and tight output clamping. This new circuit shows promise in protecting electronic systems that require a large signal bandwidth from damage by transient overvoltages.

## ACKNOWLEDGMENTS

This research was supported entirely by a contract with the U.S. Army Research Office under contract number DAAL03-87K-0078, whom we thank. We also thank L. Carpenter of the Microwave Laboratory at The Pennsylvania State University for access to a network analyzer and Touchstone software. The tests with a rectangular surge waveform were performed with equipment at the U.S. Army Harry Diamond Laboratories, Woodbridge Research Facility.

## REFERENCES

R. B. Standler, The Protection of Electronic Circuits from Overvoltages, Wiley-Interscience, New York, 434 pp., 1989

D. W. Bodle and J. B. Hayes, "Lightning Protection Circuits," U.S. Patent 2 789 254, 16 April 1957.

H M. Schlicke, "High Voltage Suppressor for Transmission Lines," U.S. Patent 3 824 431, 16 July 1974.

E. Popp, "Lightning Protection of Line Repeaters," Entwicklungs-Berichte Der Siemens-Halse-Werke, 31:25-28, Sep 1968.

O.M. Clark and R.D. Winters, "Feasibility Study for EMP Terminal Protection," General Semiconductor Industries Report TPD003 for U.S. Army Material Command, March 1973.

R. V. Garver, Microwave Diode Control Devices, Artech House, Dedham, MA, 372 pp., 1976.

J.L. Ter Haseborg and H. Trinks, "Problems Concerning EMP- and Lightning-Protection of High-Frequency Transmission Lines," IEE Conference on EMC, Surrey, IEE Publication 60, pp. 231-235, Sep 1984.

Table 1

Generic parts for circuit in Fig. 3

| | |
|---|---|
| spark gap: | 220 V dc in coaxial mount |
| R | 3.0 Ω, 1 W carbon composition |
| $D_1$ | 1N6373 6.8 V avalanche diode (transient suppressor) |
| $D_2$, $D_3$ | 1N5806 ultrafast-recovery rectifier diodes |
| $L_1$ | 27 nH, air core |
| $L_2$ | 19 nH, air core |
| $L_3$ | 62 nH, air core |
| $C_1$ | 10 pF, mica |
| $C_2$ | 20 pF, mica |

## Figure Captions

Fig. 1 Basic overvoltage protection circuit.

Fig. 2 Overvoltage protection circuit matched to impedance of transmission line, as invented by Schlicke. The varistor could be replaced by diodes.

Fig. 3 Overvoltage protection circuit designed by authors.

Fig. 4 Magnitude of forward transmission, $S_{21}$, for circuit in Fig. 3 as a function of frequency for four different dc bias voltages: 0, 2, 3, 4 V across $D_3$.

Fig. 5 Voltage standing-wave ratio (VSWR) at port 1 for circuit in Fig. 3 as a function of frequency for four different dc bias voltages: 0, 2, 3, 4 V across $D_3$.

Fig. 6 VSWR at port 2 for circuit in Fig. 3 as a function of frequency for four different dc bias voltages: 0, 2, 3, 4 V across $D_3$.

Fig. 7 Phase of forward transmission, $S_{21}$, for circuit in Fig. 3 as a function of frequency for four different dc bias voltages: 0, 2, 3, 4 V across $D_3$.

Fig. 8 Symmetrical circuit for optimal bidirectional signal propagation. This may not be a good overvoltage protection circuit, because the voltage is not tightly clamped across either port.

Fig. 9 Schematic for surge testing with 8/20 μs waveform. True differential amplifiers were used for both channels A and B to avoid errors owing to common-mode voltages.

Fig. 10 Output voltage across port 2 and input current into port 1 as a function of time. The surge begins at t = 2.4 μs; the spark gap conducts at t = 4.8 μs.

Fig. 11 Schematic for determining the response time with a rectangular waveform with a rise time of 0.6 ns. All connections were made with coaxial cable with a characteristic impedance of 50 Ω. The amplifiers for channels A and B were Tektronix model 7A29, which has a 50 Ω input impedance, in a model 7104 mainframe. Only one channel was connected for each surge in order to avoid ground loops.

Fig. 12 Digitized oscilloscope trace from the test schematic shown in Fig. 11. The voltage across port 2 is shown as a function of time. The oscilloscope display scales were 5 V/div and 5 ns/div. The transmission line was charged to 500 V.

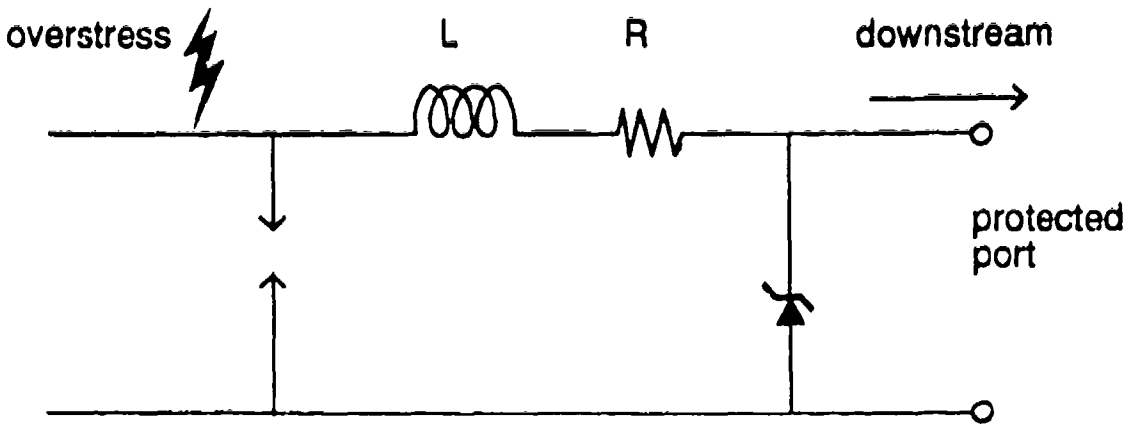


Fig. 1

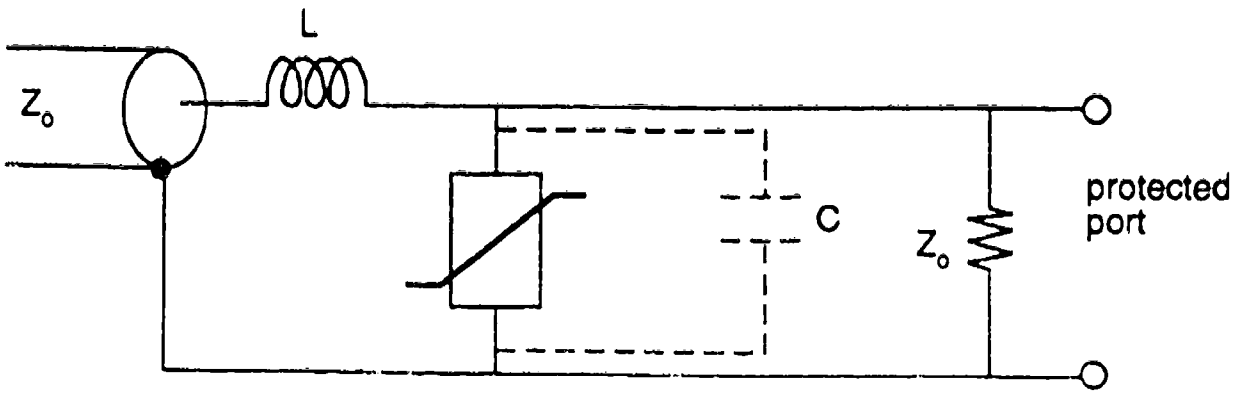


Fig. 2

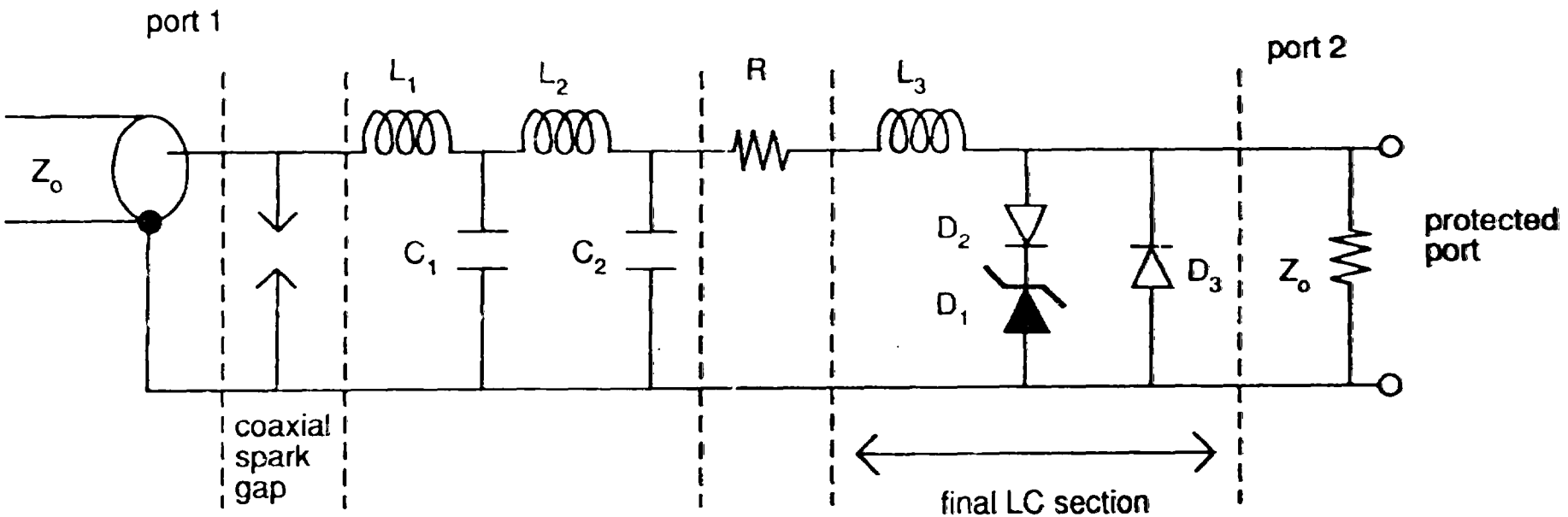
port 1
port 2
$L_1$
$L_2$
R
$L_3$
$Z_o$
$C_1$
$C_2$
$D_2$
$D_1$
$D_3$
$Z_o$
protected port
coaxial spark gap
final LC section

Fig. 3

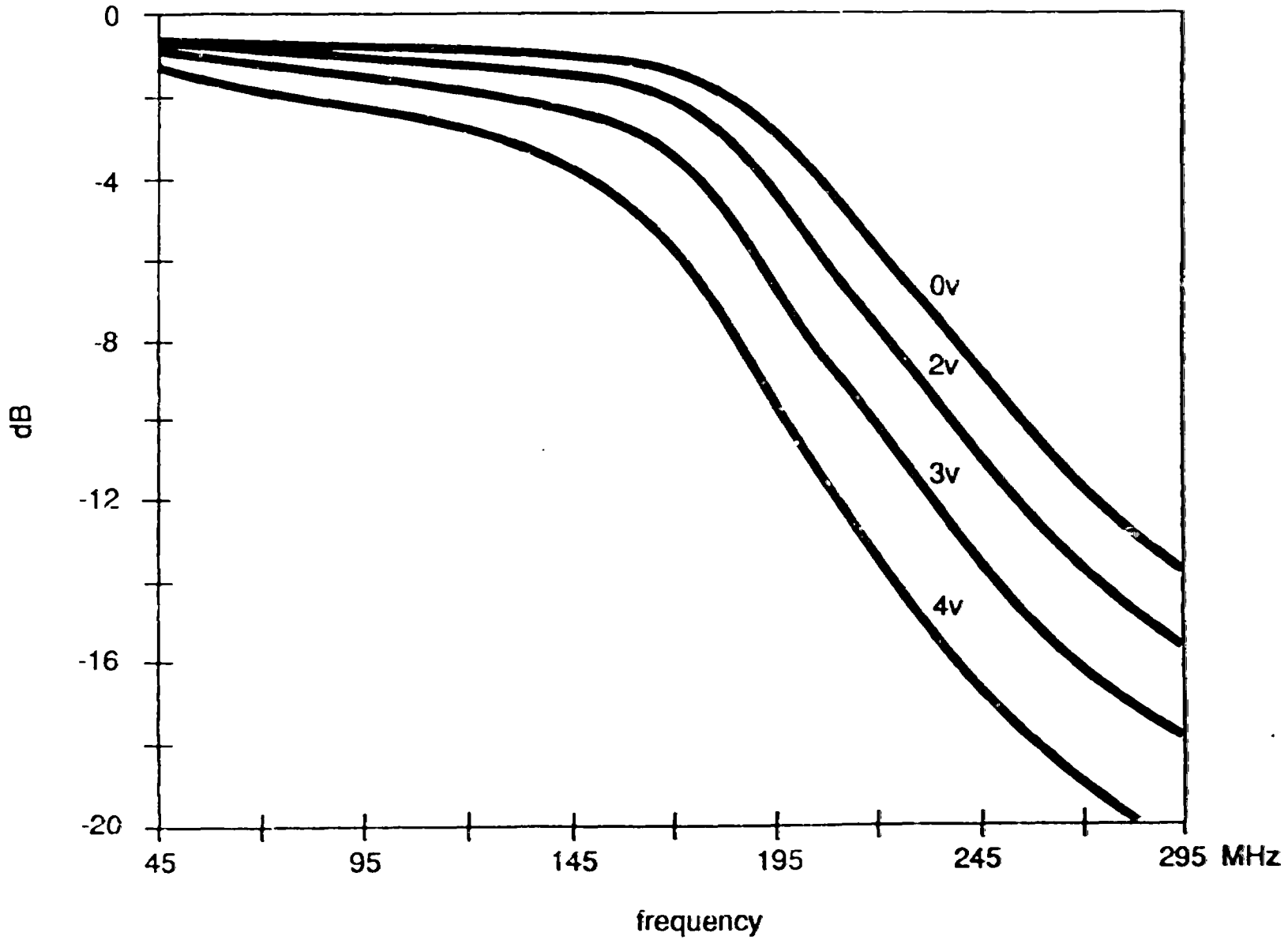


Fig. 4

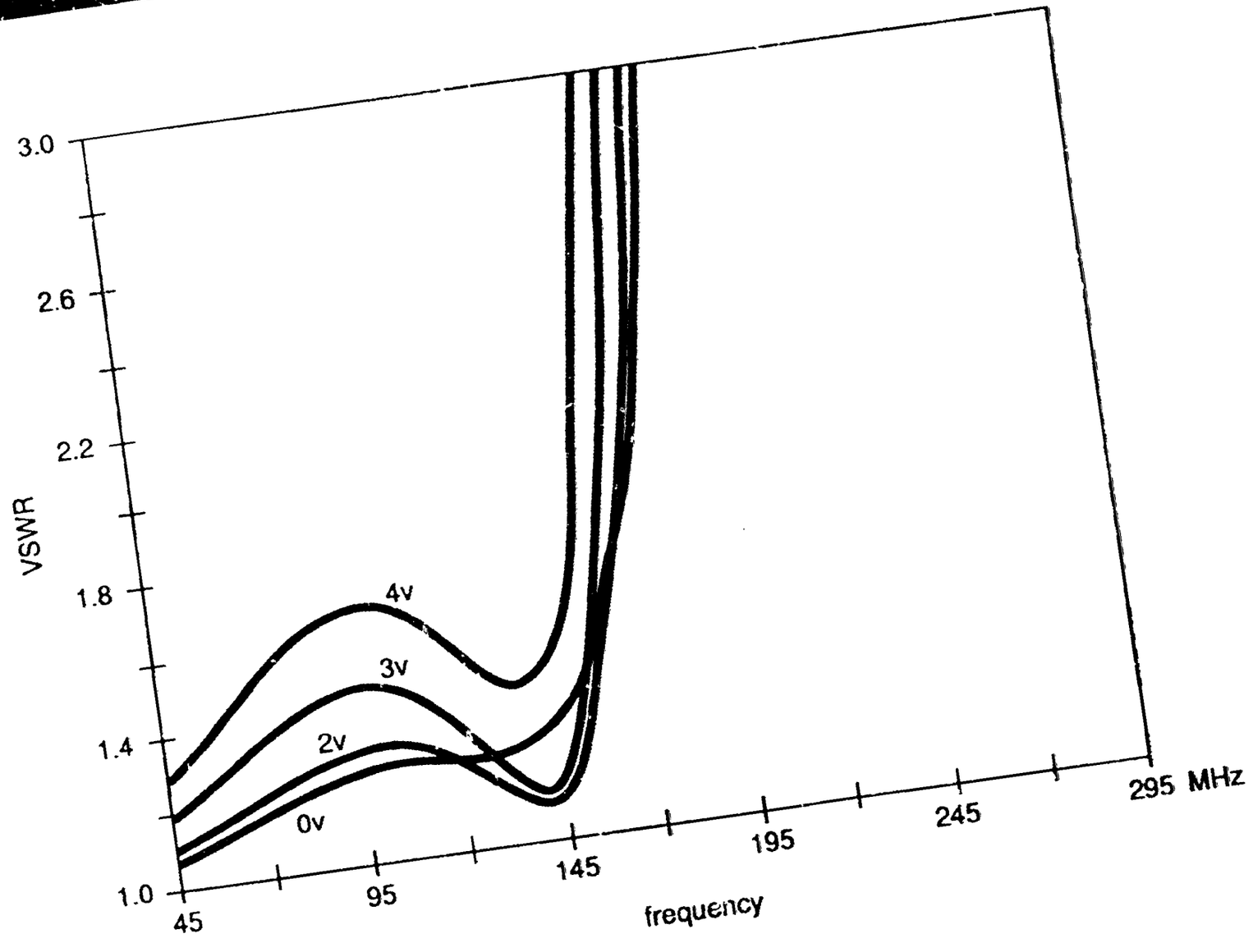
3.0
2.6
2.2
1.8
1.4
1.0
VSWR
4v
3v
2v
0v
45
95
145
195
245
295 MHz
frequency

Fig. 5

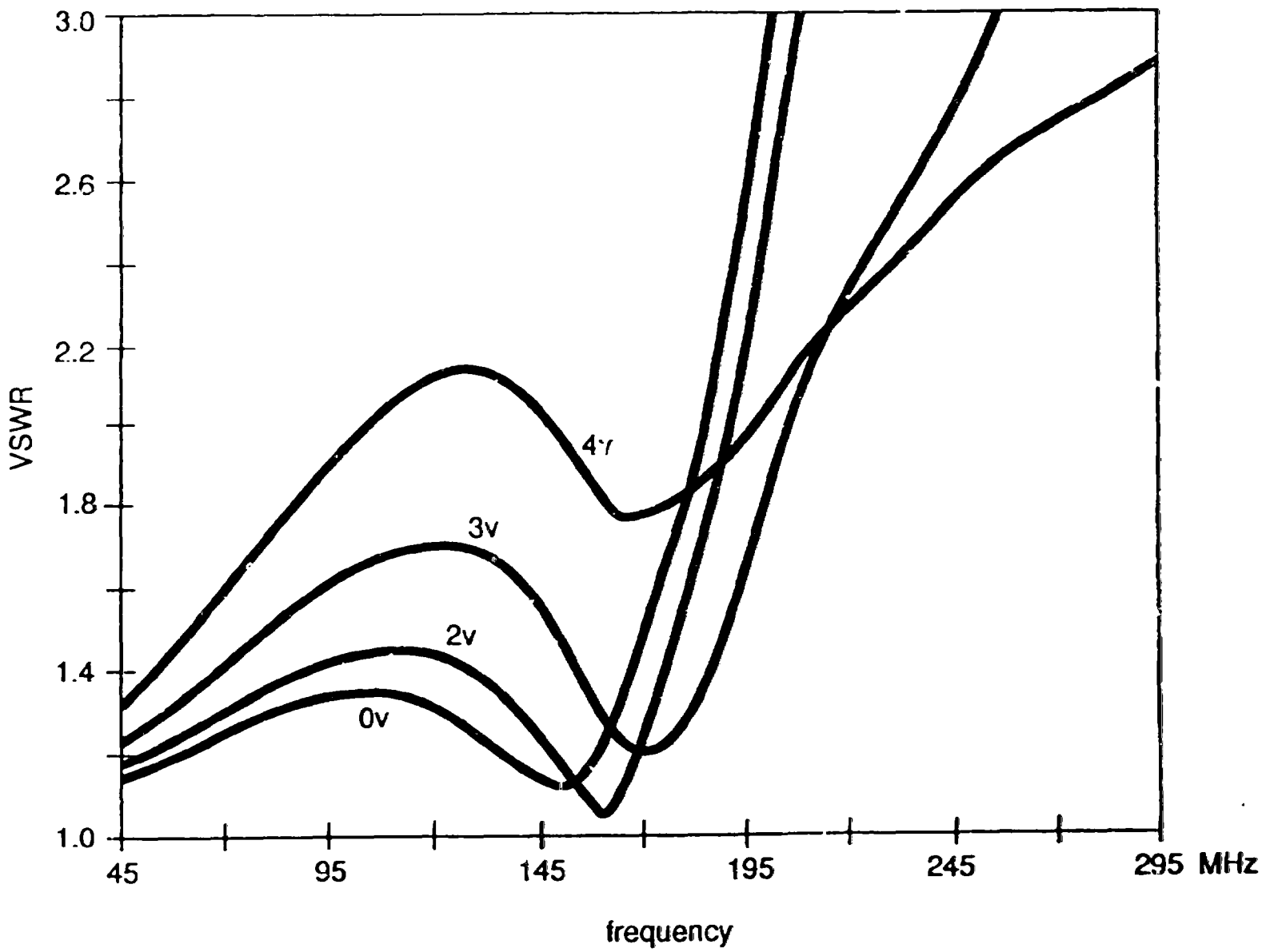
3.0
2.6
2.2
1.8
1.4
1.0
VSWR
4v
3v
2v
0v
45
95
145
195
245
295 MHz
frequency

Fig. 6

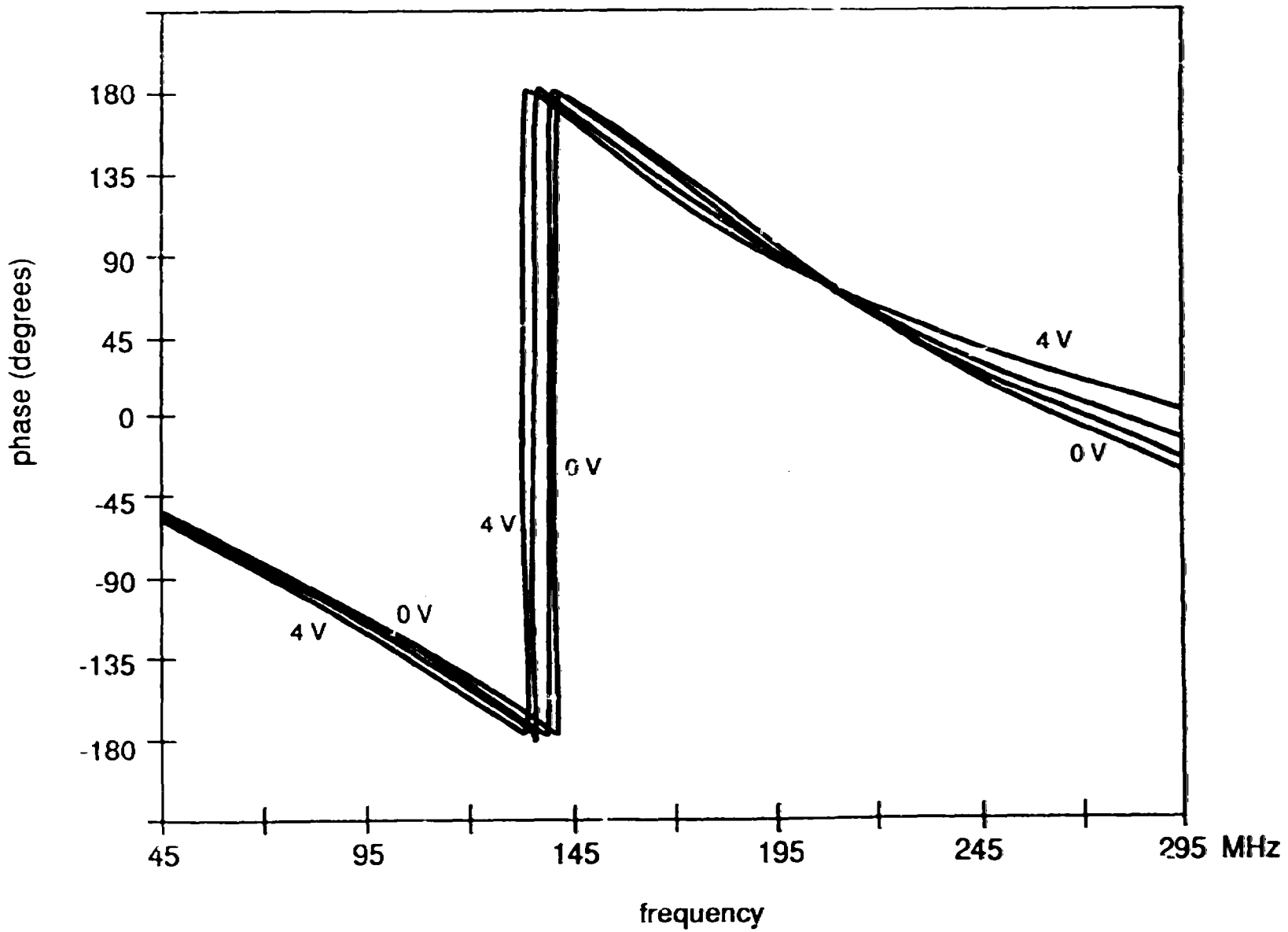
phase (degrees)
180
135
90
45
0
-45
-90
-135
-180
4 V
0 V
4 V
0 V
4 V
0 V
45
95
145
195
245
295 MHz
frequency

Fig. 7

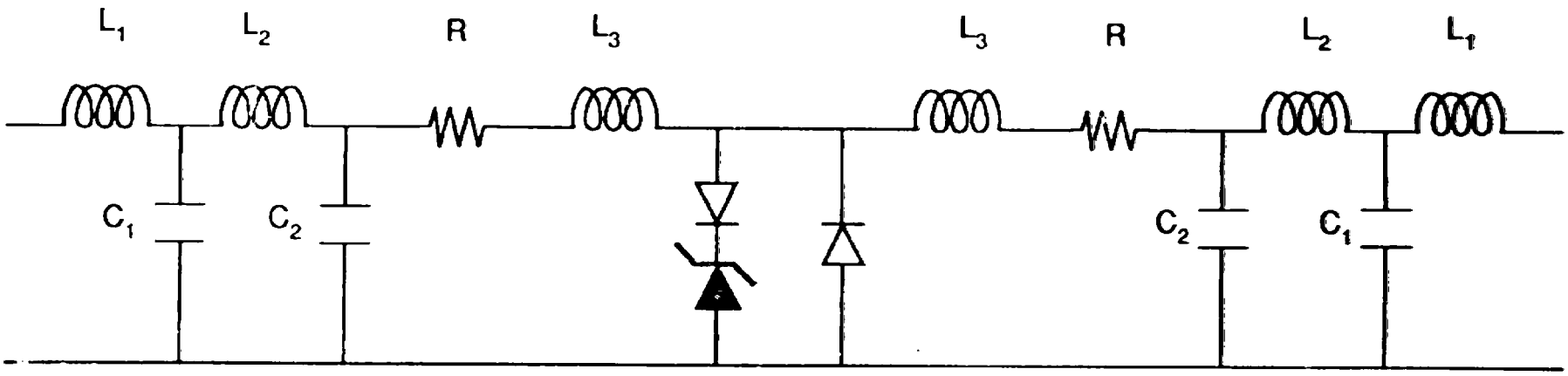


Fig. 8

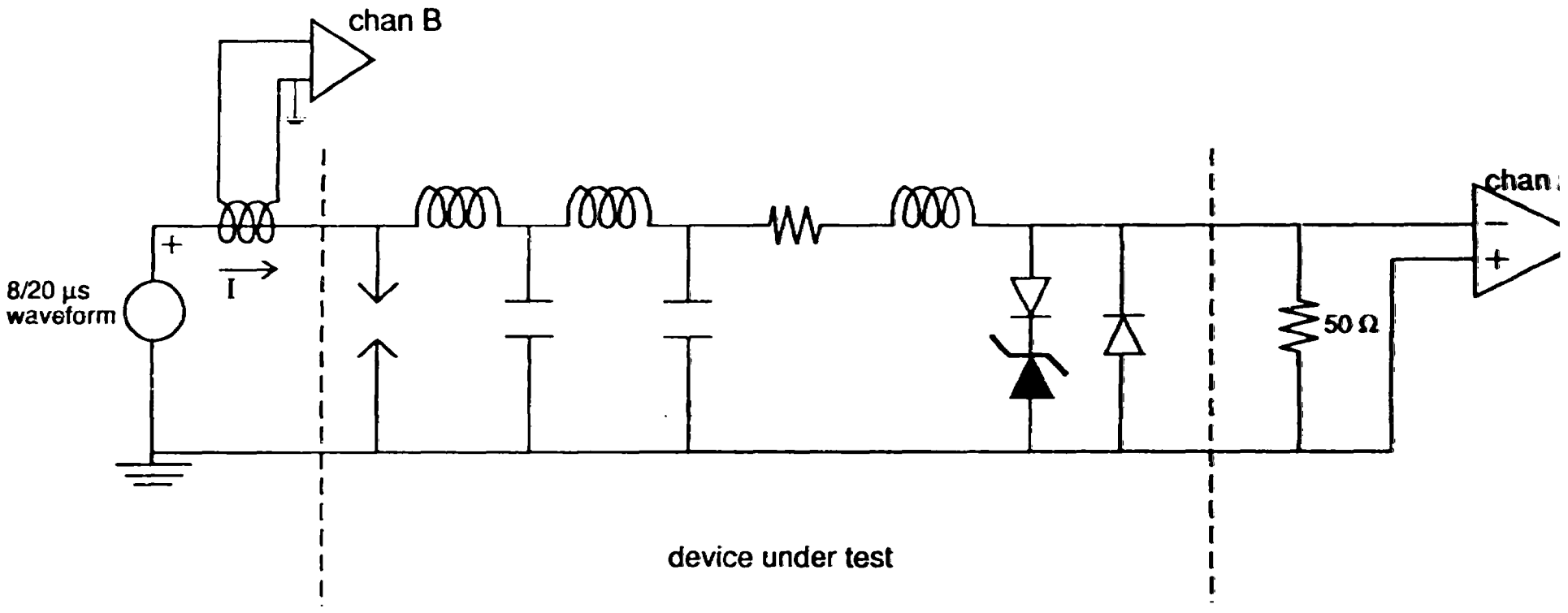


Fig. 9

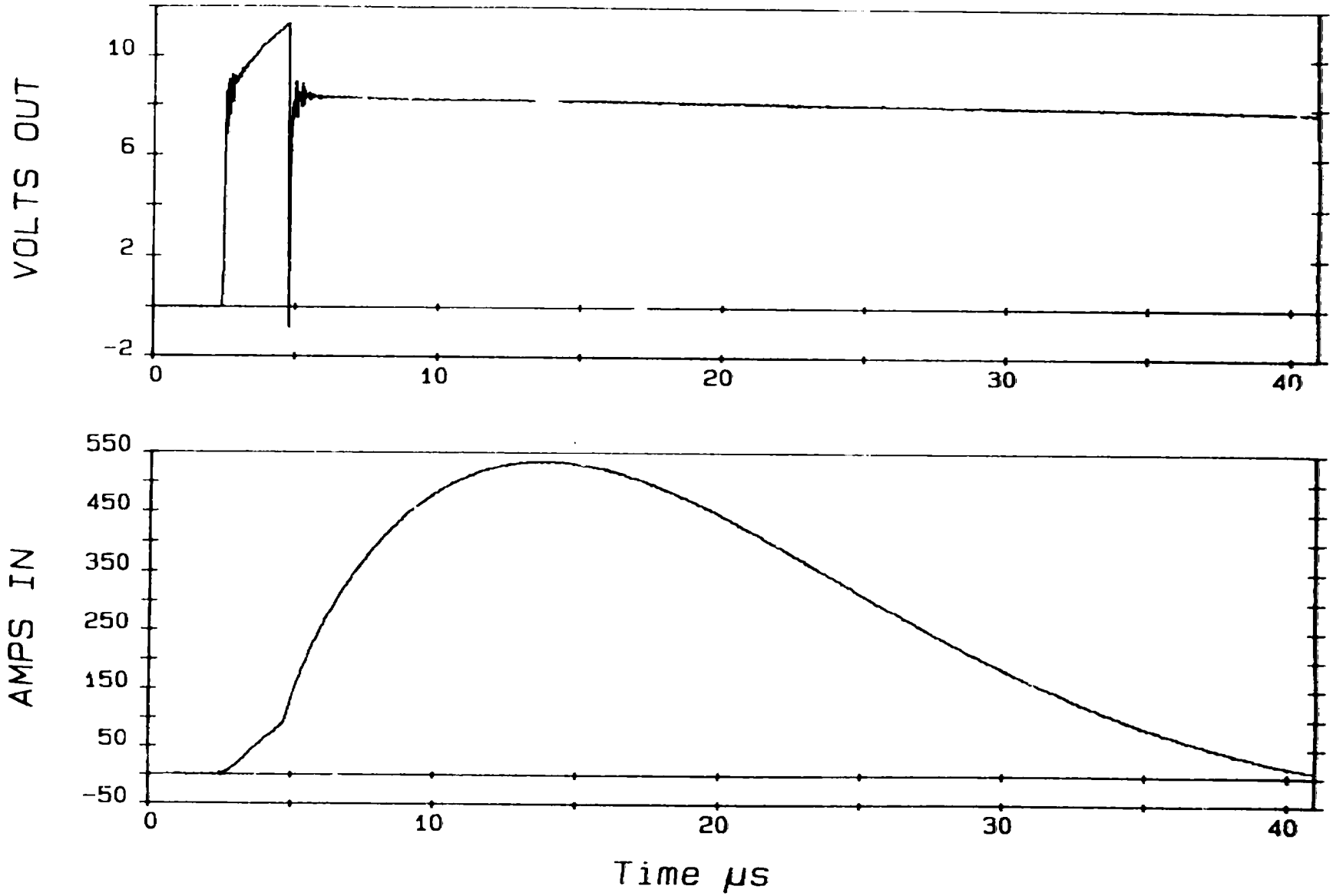
VOLTS OUT
10
6
2
-2
0
10
20
30
40
AMPS IN
550
450
350
250
150
50
-50
0
10
20
30
40
Time μs

Fig.10

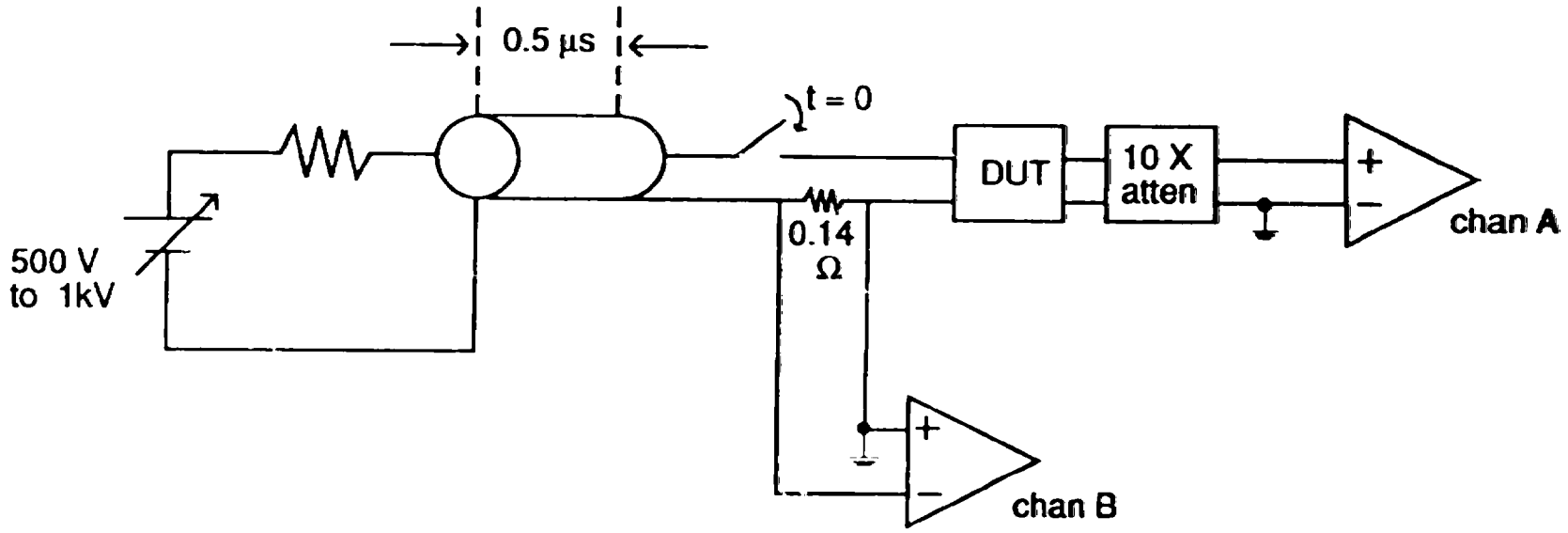


Fig. 11

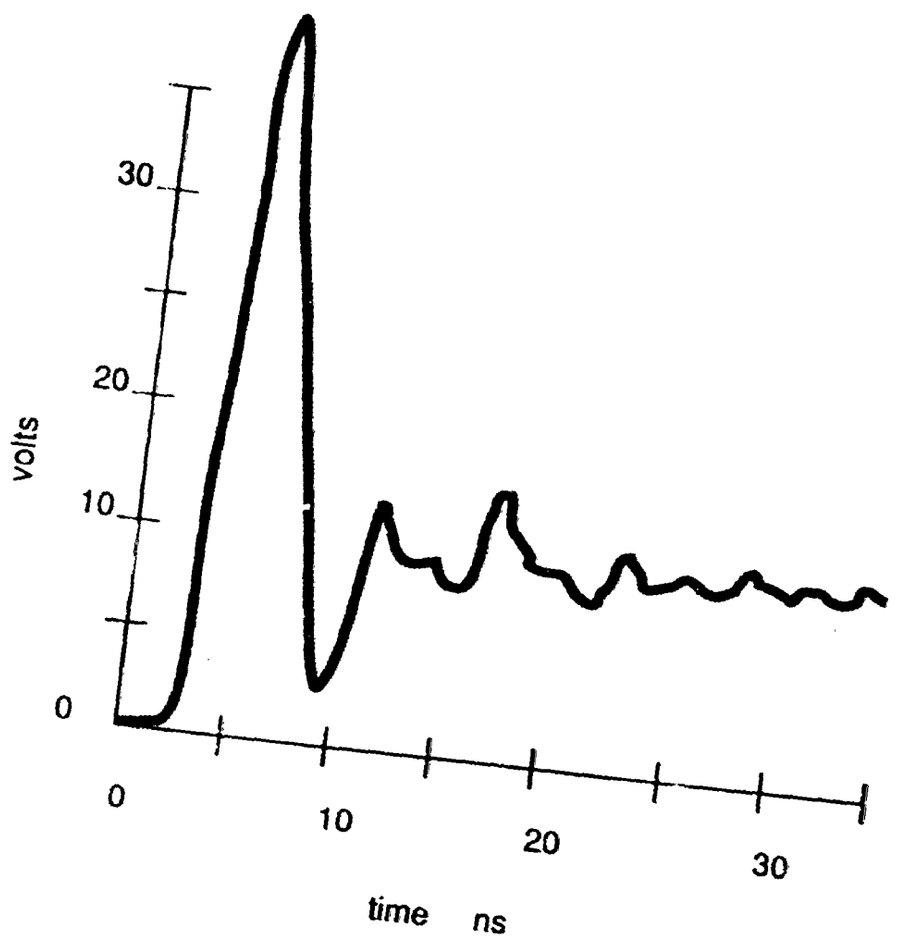


Fig. 12

IEEE National Symposium on Electromagnetic Compatibility, Denver, pp. 217-222, May 1989.

**SESSION 4C**

# CALCULATION OF ENERGY IN TRANSIENT OVERVOLTAGES

Ronald B. Standler
Department of Electrical Engineering
The Pennsylvania State University
University Park, PA 16802

## ABSTRACT

There have been many measurements of the voltage, V(t), between the hot conductor in the mains and ground. This paper considers the calculation of the energy in a transient overvoltage from the time integral of $V^2(t)/Z$, where Z has the default value of 50 Ω. Such a calculation is often used in analysis of data from recordings of transient overvoltages. There are several objections to this method: Z is a function of frequency and possibly of voltage, and this calculation does not measure the total energy in an overvoltage. A quantitative error analysis is presented that uses an artificial mains network to simulate a long branch circuit and to give the impedance of the mains as a function of frequency.

## I. INTRODUCTION

Knowledge of the energy contained in transient overvoltages, for example on the mains, is an important parameter in designing and testing circuits for protection from overvoltages. Few measurements of energy in transient overvoltages have been published. However, there are many measurements of transient overvoltages on the mains. Can one calculate the energy in an overvoltage from measurements of voltage alone by using Eq. 1?

$$W_E = \int V^2(t)/Z \, dt \qquad (1)$$

In Eq. 1, V(t) is the measured voltage as a function of time and Z is the impedance of the mains. The subscript E on $W_E$ in Eq. 1 indicates that $W_E$ is an estimate of the energy, to distinguish it from the true value of the energy, W.

One manufacturer of mains disturbance monitoring equipment prints the energy that is calculated from Eq. 1 with the default value for Z of 50 Ω, a real constant. Meissen [1] used Eq. 1 with Z = 50 Ω to find the energy content of transient overvoltages on the mains. Goedbloed [2] used

$$\int V^2 \, dt$$

as a measure of the energy, but properly stopped short of specifying a value for Z. In drafts of the revision of ANSI C62.41-1980 in 1987, W. Rhoades proposed the use of Eq. 1 with Z = 50 Ω to calculate energy from measured voltage waveforms. It certainly would be desirable if the energy could be calculated from these measurements of voltage.

There are four general areas of concern about the validity of this technique:

1. the impedance of the mains, Z, is a function of frequency,
2. Z may be a function of voltage (flashover of insulation, conduction of varistors),
3. $W_E$ does not represent the energy in the transient overvoltage, and
4. the relative location of the source of the overvoltage, other loads, and the measurement point are usually unknown during measurement of V(t).

Each of these topics is discussed in this paper. A quantitative error analysis of the use of Eq. 1 is presented, with Z = 50 Ω and several standard overvoltage test waveforms.

## II. IMPEDANCE OF THE MAINS

There have been many measurements of the impedance between either the hot or neutral conductor and the grounding conductor of the low-voltage mains [3-6]. There are several general conclusions that can be drawn from these measurements. Probably the most important is that the impedance of the mains is a function of frequency. At frequencies below about 20 kHz the value of |Z| is small, e.g. less than 5 Ω. At moderate frequencies, between about 20 kHz and 1 MHz, the impedance of the mains tends to increase as frequency increases. At high frequencies, between about 1 MHz and 20 MHz, the impedance of the mains tends to be approximately independent of frequency; the magnitude of Z can vary from about 50 Ω to about 300 Ω. The value of Z at high frequencies often contains a substantial reactive part, but the value of the reactive part depends strongly on the loads that are connected to the mains and is therefore not reproducible from site to site.

Because the impedance of the mains is a strong function of frequency, it would appear necessary to use a Fourier transform to evaluate $W_E$. One can transform V(t) to V(ω). V(ω) is then divided by Z(ω) to get the current, I(ω). The current is then transformed back to the time domain, I(t). Finally the value of

$$\int V(t) \, I(t) \, dt$$

is computed. While this is better than using Eq. 1 with a constant Z, it is still not useful for practical situations. The value of the impedance, Z(ω), is rarely known at the site of transient overvoltage measurements. Furthermore, the impedance of the mains will change with time owing to connection and disconnection of loads [7, 8].

Using Z = 50 Ω is a bad choice at frequencies below about 10 kHz, since measurements show that the actual impedance is often between about 0.4 and 5 Ω. Apparently it is not widely appreciated that common overvoltage waveforms have appreciable energy at low frequencies. The Fourier transforms, V(ω), of several common overstress test waveforms are shown in Fig. 1. These transforms were computed analytically in [9]. Fig. 1 clearly shows that most V(ω) have a relatively large value between dc and a corner frequency between 100 Hz and 100 kHz.

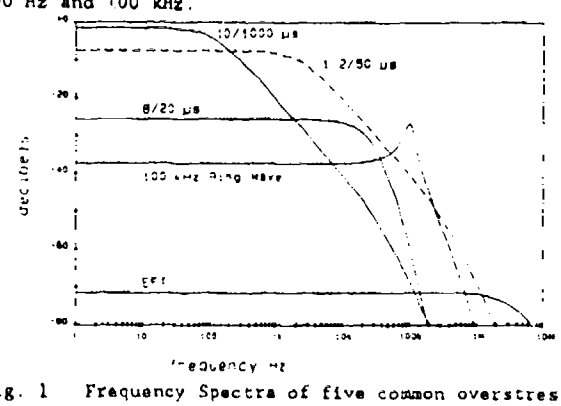


Fig. 1 Frequency Spectra of five common overstress test waveforms. The 0 dB reference level is 1 V or 1 A. The peak voltage is 6 kV for both the 1.2/50 µs and 100 kHz Ring Wave, 4 kV for the EFT, and 0.6 kV for the 10/1000 µs wave. The peak current is 3 kA for the 8/20 µs wave. The 1.2/50 µs wave is shown as a dashed line to clearly distinguish it from the others.

CH2736-7/89/0000-0217 $1.00 ©1989 IEEE

## III. Z MAY BE A FUNCTION OF VOLTAGE

When there are no surge arresters at the point of entry, lightning strikes to overhead power lines can cause flashover of insulation inside nearby buildings. Flashover of outlets on the low-voltage mains usually requires peak voltages of the order of 4 kV to 6 kV. When flashover occurs, the impedance "seen" by the transient overvoltage will decrease to less than a few ohms. It is well-known that the voltage across an arc is of the order of 20 V and is approximately independent of current. If a transient current of 100 A passes down the line, the impedance seen by the transient is 20 V/100 A, or 0.2 Ω. This value is much less than 50 Ω.

It may be argued that flashover of insulation is not common. However, the large transient overvoltages that are associated with flashovers may be associated with unusually large energy transfers from the source.

Modern electronic systems may have one or more metal oxide varistors in them to limit the voltage during transient overvoltages. These varistors may be in boxes or outlet strips that are installed specifically for protection against overvoltages, or they may be hidden inside the chassis of electronic equipment (indeed, this is good engineering practice). When the varistor conducts a current of more than $10^4$ A, the effective value of Z at the varistor will be reduced to less than 5 Ω. There are two consequences of this: (1) calculations of $W_E$ will seriously underestimate the value of the energy in the varistor, and (2) few, if any, overvoltages will be observed that have a large peak value, e.g., greater than 500 V. The second consequence has been discussed in [10].

## IV. ENERGY IN WHAT ?

Despite the problems discussed above, one might manage to properly calculate the energy from measurements of V(t) and Z(ω). One might then ask, "What is the significance of this calculation ?".

If V(t) were a voltage waveform that was propagating in one direction on a transmission line with a characteristic impedance of Z = 50 Ω, then $W_E$ would be the energy in the traveling wave at the point where V(t) was measured.

But this simple interpretation is not realistic. Most overvoltages have a duration of at least a few tens of microseconds. During this time, the voltage waveform can travel several kilometers, which is much longer than the size of most buildings. Therefore, the measured V(t) will be the sum of multiple waves, traveling in both directions, that have been reflected from discontinuities in the impedance of the transmission line, which are caused by various electrical loads on the branch circuits.

There does not appear to be a simple answer to this question about the significance of $W_E$.

Martzloff and Gruzs [11] briefly considered this issue and concluded that one could determine the energy deposited in a particular device, but could not determine the total energy in the transient overvoltage.

In a laboratory environment it is possible to measure the total energy in a transient overvoltage. The simplest way is to measure the current and voltage at the terminals of the source of the transient overvoltage. However, this technique is usually not applicable in a natural environment because (1) it is not possible to identify the location of the source or (2) it is not possible to find the conductors that contain the entire surge current.

There is yet another problem in calculating and interpreting $W_E$. In a single-phase three-wire branch circuit, for example, one may get different results from Eq. 1 if V(t) is the voltage between the hot and grounding conductors or if V(t) is the voltage between the hot and neutral conductors. The common-mode overvoltage appears between both the hot and the neutral conductors and the grounding conductor, while the differential-mode overvoltage appears between the hot and neutral conductors. It is not possible to find the total energy in an overvoltage in a three-wire circuit by measuring the potential difference between just two conductors. One must measure the potential differences between two pairs of conductors to get the complete picture, but this is rarely done in field studies of transient overvoltages.

Should the normal mains voltage be subtracted from the value of V(t) before calculating $W_E$? The two ways of calculating $W_E$ could yield significantly different results. Consider the fictitious example where V(t) is a rectangular pulse of 500 V amplitude with a duration of 10 μs. Computation of $W_E$ from Eq.1 with Z = 50 Ω gives $W_E$ = 0.05 J. However, one gets a different result if the mains voltage is subtracted from the total voltage to get the voltage "in the transient." If the same overvoltage occurs when the instantaneous value of the mains voltage is 150 V and the mains voltage is subtracted from the total, then V(t) = 350 V and one gets $W_E$ = 0.024 J, which is about 50% smaller. One can justify either method, but considering the total voltage may be preferable because that is what surge protective devices and equipment are exposed to. As a practical matter during measurements, subtraction of the normal mains voltage requires insertion of extra circuit elements (e.g., series capacitors in a high-pass filter, operational amplifiers in an active filter) that often compromise the response of the circuit above 1 MHz.

## V. IS $W_E$ A USEFUL APPROXIMATION ?

As stated in the introduction of this paper, it would be desirable to be able to estimate the energy from existing measurements of voltage during surges. In the following paragraphs the difference between $W_E$, from Eq. 1, and the true energy from the source of the overvoltage is calculated for an example of an overvoltage that propagates on one branch. An artificial mains network is used to model the impedance of the branch circuit. The effects of three different loads and four different waveforms are also considered.

### artificial mains network

In order to make reproducible measurements of conducted emissions of noise from equipment connected to the mains, it is necessary to have a standard mains impedance. Such a circuit is called an "artificial mains network" or a "line impedance stabilization network" (LISN). The official artificial mains network specified in [12-14] is shown in Fig. 2. In Fig. 2 the hot, the grounding, and the neutral conductors are labeled H, G, and N, respectively. The impedance at low frequencies is modelled by resistances of 5 Ω and 10 Ω between each line and the grounding conductor. The impedance at moderate frequencies is modelled by inductors in series with each line, together with the resistors. The constant impedance at high frequencies is modelled by a 50 Ω resistance shunted between each line and the grounding conductor. One of the 50 Ω resistances is the impedance of a voltmeter in the conventional use of the network in Fig. 2, the other 50 Ω resistance is a used to maintain the balance of the circuit.

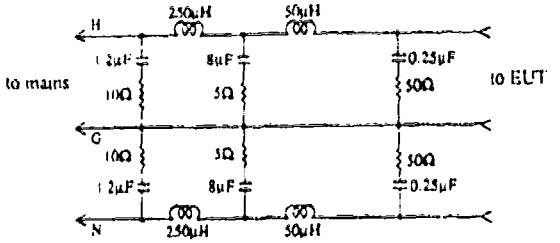


Fig. 2 The artificial mains network specified in [12-14] for use in a testing laboratory.

The network in Fig. 2 is for use in the frequency band between 10 and 150 kHz. For calculations, where parasitic effects of components are unimportant, the network should be acceptable for frequencies up to 30 MHz.

The capacitors, shown in Fig. 2, prevent the normal mains waveform, which usually has a frequency of 50 Hz or 60 Hz, from dissipating appreciable power in the shunt resistances. These capacitors cause the impedance of the artificial mains network to increase as the frequency decreases below 7 kHz, which is contrary to the actual behavior of the impedance of the mains. To use this artificial mains network in calculations of the impedance of the mains at low frequencies, it is desirable to remove the capacitors, as shown in Fig. 3.

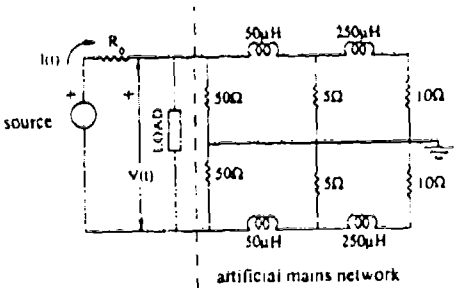


Fig. 3 Artificial mains network for use in calculations in this paper.

A plot of $Z = |V(\omega)/I(\omega)|$ as a function of frequency for steady-state sinusoidal excitation is shown in Fig. 4. This plot should be compared with Fig. 1 to appreciate that Z is not 50 Ω over most of the region where overvoltages have appreciable energy.

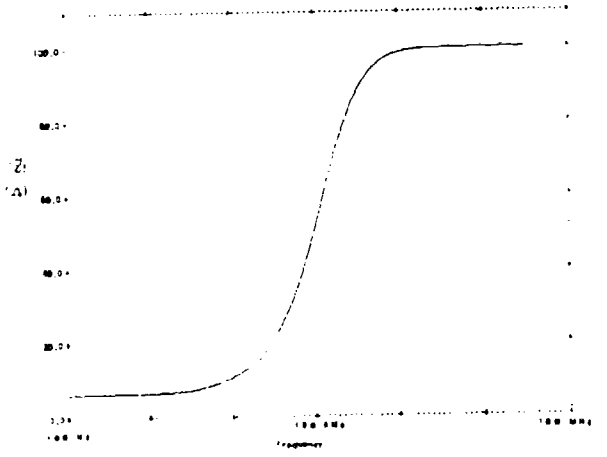


Fig. 4 Plot of |Z| vs. frequency of steady-state excitation for the circuit shown in Fig. 3. A logarithmic scale is used for frequency.

Measurements [6, 15, 16] of the characteristic impedance for propagation on the hot and neutral conductors for three-conductor cable that is commonly used in single-phase branches inside buildings give a value of about 100 Ω for propagation on the hot and neutral conductors. These measurements agree with the differential-mode impedance at high frequencies of the circuit in Fig. 3.

The network in Fig. 3 is only used for calculations of differential-mode voltages because no inductance is shown in the grounding conductor. In the conventional use of an artificial mains network to measure conducted noise from equipment, inductance in the grounding conductor is not necessary, since the ground is a metal plane on a laboratory bench.

## sources and loads

The most favorable situation for comparing $W_E$ to the true energy delivered by a transient overvoltage occurs when the source of the overvoltage is contiguous to the points where V(t) is measured. This situation will be discussed first, later a more realistic situation will be discussed.

In the schematic of Fig. 3, the source of the overvoltage is represented by a Thevenin equivalent circuit, where $R_o$ is the output resistance of the voltage source. Four different standard overvoltage test waveforms were used:

1. a single pulse from the IEC 801-4 electrical fast transient (EFT),
2. the 100 kHz Ring Wave defined in ANSI C62.41-1980,
3. the 1.2/50 μs voltage waveform, and
4. the 10/1000 μs waveform.

The EFT has a duration of 0.05 μs and represents a single pulse in a showering arc, such as generated by switching an inductive load with moving switch contacts. The 100 kHz Ring Wave represents overvoltages that are commonly observed on branch circuits inside buildings. The 1.2/50 μs waveform is the standard lightning overstress. The 10/1000 μs waveform is used to simulate overvoltages that have long durations.

Three different loads were used during the calculations:

1. no load (open circuit),
2. 6 mH + 40 Ω, and
3. 0.2 μF || 200 Ω.

Vines et al. [6] reported that a 3/4 horsepower induction motor had an impedance of 40 + 188j Ω at 5 kHz, which was the inductive load used in these calculations. The capacitive load used in these calculations was an approximate characterization of a small television receiver.

The error caused by different values of the impedance of the mains and a load can be estimated by the following calculations.

## calculation of error

The true energy transferred from the source, W, is calculated from Eq. 2, where V(t) is the voltage across the load and I(t) is the current through the source when the artificial mains network and the load are connected.

$$W = \int V(t)\, I(t)\, dt \qquad (2)$$

The estimated energy, $W_E$, is calculated with Eq. 1 and Z = 50 Ω, where V(t) is the voltage across the load when the artificial mains network and the load are connected as shown in Fig. 3. The current and voltage were calculated by the circuit simulation program

Table 1
True and Estimated Energy in
differential-mode Overvoltage

| Overvoltage Waveform and Load Impedance | True Energy W | Estimated Energy $W_E$ | Ratio $W/W_E$ |
|---|---|---|---|
| 5/50 ns EFT waveform, 4 kV peak, $R_o$ = 50 Ω | | | |
| no load | 2.7 mJ | 5.2 mJ | 0.507 |
| 6 mH + 40 Ω | 2.7 mJ | 5.2 mJ | 0.507 |
| 0.2 μF \|\| 200 Ω | 41 μJ | 30 μJ | 1.36 |
| 0.5 μs-100 kHz ring waveform, 6 kV peak, $R_o$ = 12 Ω | | | |
| no load | 0.81 J | 1.3 J | 0.606 |
| 6 mH + 40 Ω | 0.81 J | 1.3 J | 0.606 |
| 0.2 μF \|\| 200 Ω | 0.41 J | 0.46 J | 0.896 |
| 1.2/50 μs waveform, 6 kV peak, $R_o$ = 3 Ω | | | |
| no load | 82.3 J | 14.2 J | 5.80 |
| 6 mH + 40 Ω | 83.7 J | 13.8 J | 6.08 |
| 0.2 μF \|\| 200 Ω | 84.1 J | 13.8 J | 6.08 |
| 10/1000 μs waveform, 800 V peak, $R_o$ = 10 Ω | | | |
| no load | 11.1 J | 1.4 J | 7.82 |
| 6 mH + 40 Ω | 10.7 J | 1.2 J | 8.90 |
| 0.2 μF \|\| 200 Ω | 11.0 J | 1.4 J | 8.07 |

PSPICE, version 3.06. The value of W was calculated by a trapezoidal rule integration using the values of V and I from the PSPICE program. The results are given in Table 1. The ratio $W/W_E$ is useful as a correction factor: when $W_E$ is multiplied by this factor, one obtains the true energy from the output terminals of the source.

The results are easy to interpret. First, consider the EFT waveform. When the load has a large impedance at high frequencies (no load, motor load), the value of $W_E$ is about twice the value of W. By inspection of Fig. 3, it is easy to see that the differential-mode impedance seen by high frequency terms from the source is 100 Ω, not 50 Ω used in the calculation of $W_E$. This ratio of values of Z accounts for the fact that $W/W_E$ is not unity. The problem is not in the circuit chosen for Fig. 3, since this differential-mode impedance agrees well with measurements of actual branch circuits, as discussed above. When the load has a small impedance at high frequencies (e.g., 0.2 μF load), the value of $W_E$ tends to be smaller than W.

For a long duration waveform, such as the 10/1000 μs wave, the impedances of the 50 μH and 250 μH series inductances in Fig. 3 are negligible compared to the resistance values. The differential-mode impedance has a low-frequency limit of 6.25 Ω, which is a factor of 1/8 of the 50 Ω value used in the computation of $W_E$. This ratio of impedances accounts for most of the ratio of $W/W_E$.

The results for the moderate duration waveforms fall between the two limiting cases of the EFT and 10/1000 μs waveforms.

Where the source of the overvoltage is contiguous to the measurement point and there are no varistors or flashover, the ratio of $W/W_E$ is between 0.5 and 9 for the 12 cases presented in this paper. While these correction factors might seem to indicate that $W_E$ could be used as a crude estimate of W, these factors were obtained from the unrealistic assumption that the measuring point for V(t) was contiguous to the source of the overvoltage and that there were no reflections.

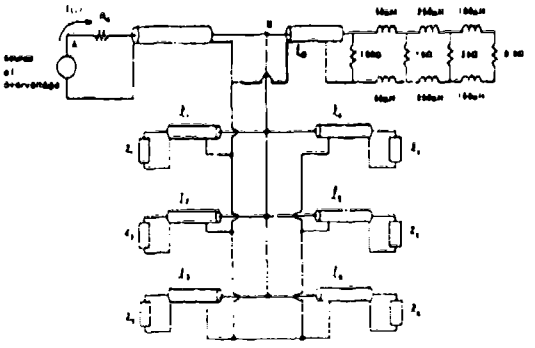

Fig. 5 Simple representative circuit diagram for propagation of overvoltages inside a building. The cylinders represent ideal transmission lines with a characteristic impedance of 100 Ω.

source on different branch than voltage measurement

When the source of the overvoltage is unknown, the measured voltage data would rarely come from a point that was contiguous to the source as in Fig. 3. A more typical situation is shown in Fig. 5. An overvoltage source is located at point A on one branch. There are six other branches, which are terminated by loads $Z_1$ through $Z_6$. Point B in Fig. 5 represents distribution panel in the building where the overvoltage originated. The voltage V(t) is measured across the load on one of the branch circuits.

When the overvoltage reaches point B, it splits into eight parts. One part propagates out of the building into the utility network. One part is reflected back toward the source of the overvoltage by the discontinuity in impedance at point B. The other six parts propagate on the transmission lines that represent the branch circuits inside the building.

The utility network may be modeled by the artificial mains network shown in Fig. 3, with two changes. (1) The output impedance of the utility network at low frequencies (i.e., < 1 kHz) is modelled by a 0.4 Ω resistance and a total inductance of 800 μH as described in [17]. A conventional artificial mains network for laboratory use has such a small differential-mode component when the mains are connected to the network. (2) Because only differential-mode voltages are considered, the connections to earth in Fig. 3 are deleted in Fig. 5.

The pair of 50 Ω resistors in the artificial mains network that account for the characteristic impedance of the cable at high frequencies match the 100 Ω characteristic impedance of the transmission line. This prevents reflections of high-frequency information at the junction between the continuous and lumped-element representations of the transmission line.

Waves on the transmission lines are reflected from impedance discontinuities presented by loads that are connected to the branch circuits. The multiple reflections in this type of network will generate an oscillatory voltage waveform across each load, even when the original overvoltage is unipolar [9]. In the limit of long times, the transmission lines may be neglected: steady-state circuit analysis will be adequate [9, 15] to describe the voltages, currents, and energy in Fig. 5.

For simplicity, only one load is shown on each branch circuit and no additional buildings are shown connected to the utility network in Fig. 5, although these additional features may be necessary for a realistic calculation.

In order to make an accurate estimate of energy from measurements of V(t), it would be desirable to obtain a correction factor, $W/W_E$, from calculations of voltages and currents in a representative circuit, such as the one shown in Fig. 5. However, this is not feasible since both the length of the branch circuits and the complex impedance of the loads that were connected to the mains in the building where V(t) was measured are usually unknown.

## VI. MEASUREMENT OF ENERGY DEPOSITED IN VARISTORS

Attempts to estimate energy from transient overvoltages across unspecified branch circuits may be desirable in order to get as much information as possible from previous measurements of rare overvoltages. However, future measurements of overvoltages across the mains should be done with a representative protective device, such as a metal oxide varistor, at the measurement point. It is no longer in doubt that overvoltages exist. Numerical data are now needed on how to use appropriate devices to protect vulnerable systems from overvoltages.

Standler [18] described an experiment to determine the energy absorbed in metal oxide varistors that are connected across the mains as shown in Fig. 6. Both the current and voltage are measured in each varistor with a four-channel digital oscilloscope. (This experiment is now entering its third year; results will be published in future papers.)

In addition to being a relevant experiment, using varistors at the measuring point can prevent damage to the instrumentation by transient overvoltages. The varistors also can be used to compress the voltage scale so that common events are in the middle of the voltage range, while rare events that have a large energy are not beyond the full-scale voltage.

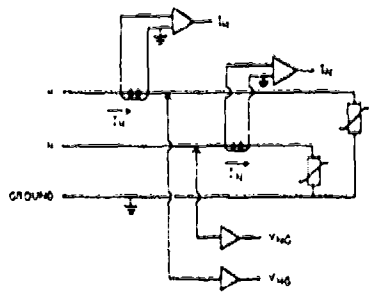


Fig. 6 Circuit diagram for experiment to measure energy deposited by overvoltages in two metal oxide varistors connected to the mains. A pair of current transformers and digital oscilloscopes measure the currents in the hot and neutral conductors, $I_H$ and $I_N$. A pair of voltage probes and digital oscilloscopes measure the voltages between the hot and grounding conductors, $V_{HG}$, and between the neutral and grounding conductors, $V_{NG}$.

There are several reasons why the energy dissipated in a varistor will be less than the total energy in the surge. Some of the energy in the surge will propagate on other branches and may be absorbed in other varistors and resistive loads elsewhere in the building. Some of the transient voltage will appear across the resistance of the building wiring and dissipate energy in the resistance of the wire. While the varistor will prevent flashover at the measurement point, it is possible that flashover might occur upstream from the varistor. The measured energy in the varistor is a lower bound for an estimate of the total energy in the surge.

It would be desirable to increase the fraction of surge current that is measured, and thus make the energy that is measured in the varistor be a better approximation for the total energy in the surge. There are two ways to do this. (1) For experimental purposes, one might choose varistors with the smallest clamping voltage that will not conduct appreciable current during normal mains operation. This may decrease the magnitude of the current in other surge protective devices that may be in the environment. (2) The varistors should be mounted near the circuit breaker panel at the point of entry. On average, the distribution panel is the closest point to a source on an unspecified branch. Overvoltages that propagate toward the point of entry will "see" the varistors before appreciable overvoltages propagate away from the distribution panel on other branches of the circuit.

## VII. CONCLUSIONS

In the introduction of this paper the question was posed: "Can one calculate the energy in an overvoltage from measurements of voltage alone ?"

Where the source of the overvoltage is contiguous to the measurement point and there are no varistors or flashover, calculating $W_E$ with Z = 50 Ω could be used as a crude estimate of W. However, the assumption that the measuring point for V(t) was contiguous to the source of the overvoltage is unlikely to be valid in most situations. When the source and the measurement point are on different branches, $W_E$ is not a good approximation for W. This alone makes the calculation of energy from measurements of voltage alone an unreliable operation. Consideration of flashover and the effects of surge protective devices in the environment will further weaken the relationship

between W and $W_E$. Furthermore, the common-mode and differential-mode voltages are irretrievably mixed in any measurement of a single voltage difference in a three-wire system, which further complicates the interpretation of $W_E$ in these situations.

The total energy in the transient overvoltage is still of interest as a "worst-case" exposure for a protective device. However, as explained in this paper, there is little hope of being able to accurately determine the total energy in a transient overvoltage except in a laboratory environment.

A method for measuring energy dissipated in a varistor is advocated for use in future experiments. While measuring the energy in a varistor avoids many of the problems associated with $W_E$, the energy dissipated in a varistor is also an underestimate of the total energy in the transient overvoltage.

## ACKNOWLEDGMENTS

It is a pleasure to acknowledge helpful discussions with F.D. Martzloff, P. Richman, R.M. Showers, and D. Shakarjian. This work was supported by contracts from the U. S. Army Research Office and the Allegheny Power System.

## REFERENCES

[1] W. Meissen, "Transiente Netzüberspannungen," Elektrotech. Z., 107:50-55, 1986.

[2] J.J. Goedbloed, "Transient in Low-Voltage Supply Networks," IEEE Trans. EMC, 29:104-115, May 1987.

[3] J.H. Bull, "Voltage Spikes in L.V. Distribution Systems and their Effects on the Use of Electronic Control Equipment," Report Nr. 5254, Electrical Research Association, Leatherhead, Surrey, 1968.

[4] J.R. Nicholson and J.A. Malack, "RF Impedance of Power Lines and Line Impedance Stabilization Networks in Conducted Interference Measurements," IEEE Trans. EMC, 15:84-86, May 1973.

[5] J. A. Malack and J.R. Engstrom, "RF Impedance of United States and European Power Lines," IEEE Trans. EMC, 18:36-38, Feb 1976.

[6] R.M. Vines, H.J. Russell, K.C. Shuey, and J.B. O'Neal, "Impedance of the Residential Power-Distribution Circuit," IEEE Trans. EMC., 27:6-12, Feb 1985.

[7] J.R. Nicholson and J.A. Malack, "Reply to Comments by R.A. Southwick", IEEE Trans. EMC., 15:199, Nov 1973.

[8] R.A. Piety, "Intrabuilding Data Transmission Using Power-Line Wiring," Hewlett-Packard Journal, 38:35-40, May 1987.

[9] R.B. Standler, Protection of Electronic Circuits from Overvoltages, Wiley-Interscience, New York, 429 pp., 1989.

[10] F.D. Martzloff, "Discussion of: Rural Alaska Power Quality by Aspnes, Evans, and Merritt," IEEE Transactions on Power Apparatus and Systems, 104:618-9, March 1985.

[11] F.D. Martzloff and T.M. Gruzs, "Power Quality Site Surveys: Facts, Fiction, and Fallacies," IEEE Industry Applications Society Industrial and Commercial Power Conference, Nashville, TN, pp. 21-33, May 1987.

[12] American National Standard C63.4-1981, "Methods of Measurement of Radio-Noise Emissions from Low-Voltage Electrical and Electronic Equipment in the Range of 10 kHz to 1 GHz."

[13] C.I.S.P.R 16, "Specification for Radio Interference Measuring Apparatus and Measuring Methods," 1987.

[14] VDE 876-1, "Geräte zur Messung von Funkstörungen," 1978.

[15] F.D. Martzloff, "The Propagation and Attenuation of Surge Voltages and Surge Currents in Low-Voltage AC Circuits," IEEE Trans. Power Apparatus and Systems, 102:1163-1170, May 1983.

[16] R.B. Standler and A.C. Canike, Mitigation of Mains Disturbances, U. S. Air Force Weapons Laboratory TR-86-80, 192 pp.

[17] IEC Publication 725, "Considerations on Reference Impedance of Use in Determining the Disturbance Characteristics of Household Appliances and Similar Electrical Equipment," 1981.

[18] R.B. Standler, "An Experiment to Monitor Disturbances on the Mains," IEEE Industry Applications Society Conference, Atlanta, GA, pp. 1325-1330, Oct 1987.